revealing co-enrichment of inflammatory and neurodegeneration-related programs, consistent with known connectivity patterns. These findings establish a biological foundation for biomarker validation studies and inform precision medicine strategies in pediatric neurotrauma.

Keywords Traumatic brain injury, Pediatrics, Critical care medicine, Proteomics, Bioinformatics, Machine learning

Introduction

Pediatric severe traumatic brain injury (sTBI) remains a leading cause of death and long-term neurocognitive disability, with survivors often experiencing persistent deficits that evolve across development (Weil and Karelina 2019). Although the initial mechanical insult initiates injury, secondary processes, including neuroinflammation, blood–brain barrier disruption, excitotoxicity, oxidative stress, and progressive axonal and synaptic injury, largely drive outcome (Serpa et al. 2021; Lindblad et al. 2021; Zhang et al. 2021). These processes unfold within the context of an actively developing brain, rendering pediatric sTBI biologically distinct from adult injury and limiting the applicability of adult-derived biomarkers and mechanistic frameworks. Thus, pediatric sTBI reflects specific pathophysiological responses that require age-appropriate research paradigms (Walker et al. 2009; Figaji 2017).

Progress in pediatric sTBI has been limited by an incomplete molecular understanding of injury pathobiology. Conventional clinical grading systems, neuroimaging, and single-analyte biomarkers provide limited mechanistic insight and fail to capture the biological heterogeneity characterizing pediatric brain injury (Maas et al. 2022; Tenovuo et al. 2021). While blood-based biomarkers offer a minimally invasive window into central nervous system pathology (Fraser et al. 2011; Abu Hamdeh et al. 2021; Chen et al. 2019, 2021), many brain-derived proteins circulate at extremely low concentrations and remain below the detection limits of traditional proteomic platforms (Chen et al. 2021; Cui et al. 2024). Moreover, prior studies have largely focused on inflammatory mediators or a limited set of established neuronal markers.

Recent advances in ultra-sensitive proteomics now enable detection of low-abundance brain-associated proteins in peripheral blood. The nucleic acid-linked immuno-sandwich assay (NULISA) achieves unprecedented attomolar protein detection (Feng et al. 2023); however, it has yet to be applied to characterizing pediatric sTBI pathobiology. This technology permits the quantification of 120 proteins with the CNS Disease Panel, across distinct domains of neuropathology, including amyloid/tau pathologies, synaptic/synuclein regulation, neurodegeneration, vascular/metabolic proteins, and neuroinflammation (Zhang and Xu 2025; Li et al. 2025). This breadth enables systems-level interrogation of acute pediatric sTBI pathobiology, providing early insight into preferentially disrupted neural domains.

In this exploratory, hypothesis-generating case–control study, we applied ultra-sensitive plasma proteomic profiling using the NULISA platform to measure plasma proteins during the acute phase of sTBI. By comparing age- and sex-matched healthy controls with sTBI patients upon pediatric intensive care unit (PICU) admission (Day 1) and shortly thereafter (Day 3), we aimed to (1) identify changes in differentially expressed brain- and inflammation-associated proteins in pediatric sTBI, (2) define their temporal evolution during the acute injury phase, and (3) delineate protein–protein interaction (PPI) networks and clinical associations. This study represents the first application of the NULISA platform to severe pediatric traumatic brain injury, leveraging a high-dimensional, large-scale proteomic panel spanning multiple CNS-specific protein domains to generate mechanistic insight, enable biomarker discovery, and inform precision-oriented therapeutic strategies.

Methods

Study design and participants

Patients with sTBI were recruited from the Children's Hospital, London Health Sciences Centre (London, Ontario, Canada), the regional pediatric Level 1 trauma center for Southwestern Ontario. LHSC serves a catchment area of 190,000 km^2 with a pediatric population exceeding 80,000 children. We included 23 previously healthy pediatric patients (age < 18 years) admitted to the PICU after sustaining sTBI, defined as a pre-sedation Glasgow Coma Scale (GCS) score ≤ 8 and Maximum Abbreviated Injury Scale head (MAIS head) score ≥ 4 (Stewart et al. 2013; Alharfi et al. 2013, 2014; Alofisan et al. 2019; Hochstadter et al. 2014). Injury data were obtained from LHSC's trauma registry, which contains detailed demographic, injury, clinical, and outcome data on pediatric sTBI patients as part of the Ontario Trauma Registry's Comprehensive Data Set (age, weight, sex, etiology of TBI, injury severity score, presenting GCS, pupillary findings, incidence of hypotension, requirement for emergent neurosurgical interventions, and clinical outcomes). Injury diagnoses, including cerebral edema and midline shift, were defined based on CT scan abnormalities systematically recorded in LHSC's trauma registry, interpreted by attending neuroradiologists with specialized training in brain injury imaging.

Age- and sex-matched healthy controls were recruited from an outpatient clinic. This sample size is consistent with published pediatric exploratory proteomic studies (Miller et al. 2021; Patel et al. 2024; Spagnolo et al. 2025; Stranges et al. 2025). Our 'Day 3' timepoint represents a pragmatic sampling window spanning Days 3–5 post-injury, reflecting the clinical constraints of a critically ill pediatric cohort. Of the samples collected within this window, the majority were obtained on Day 3, with 2 collected on Day 4 and 2 on Day 5 (median Day 3, IQR 0). Formal power calculations were not feasible due to the absence of prior effect size estimates.

Age, sex, and timepoint were retained across both heatmaps to provide a consistent clinical reference frame and enable interpretation of protein trajectories in the context of key demographic and temporal variables. Regarding APOE4 carrier status, we included this variable given its well-established role in amyloid pathology and its association with unfavorable outcomes following TBI (Liu et al. 2017; Johnson et al. 2010; McFadyen et al. 2021), making it a biologically relevant covariate in the context of our amyloid/tau domain findings.

Blood collection and processing

Blood samples for proteomic analyses and routine laboratory testing were collected on PICU admission (Day 1) and on PICU Day 3 (Supplemental Fig. 1). For patients without a Day 3 sample, specimens collected on Day 4 ($n = 2$) or Day 5 ($n = 2$) were incorporated into the "PICU Day 3" timepoint (median Day 3, IQR 0). Certified nursing personnel collected samples into citrate-containing tubes (Vacutainers; BD Biosciences, Mississauga,

A

Admission variables	Statistics
Age (years 1-17), median (IQR)	15 (10)
Weight (Kg), median (IQR)	58 (48)
Male, n (%)	16 (70%)
Etiology- All Blunt Mechanism of Injury	
MVC, n (%)	16 (70%)
Fall, n (%)	3 (13%)
Intentional, n (%)	1 (4%)
Other, n (%)	3 (13%)
Injury severity score, median (IQR)	33 (9)
Injury profile, median (IQR)	
MAIS HEAD	5 (0)
MAIS NECK	1 (0)
MAIS Face	1 (1)
MAIS Thorax	3 (0.75)
MAIS Abdomen	2 (0)
MAIS Spine	2 (1.5)
MAIS Upper extremity	2 (0.25)
MAIS Lower extremity	2 (1)
MAIS External	1 (0)
Pre-sedation GCS, median (IQR)	4 (2)
Pre-sedation motor GCS, median (IQR)	1 (1)
Bilateral fixed pupils , n (%)	8 (35%)
Hypotensive episode, n(%)	8 (35%)
Emergent surgical intervention, n (%)	3 (13%)
Outcomes	
Mortality, n (%)	7 (30%)
Ventilator free days, median (IQR)	22 (30)
For survivors only (n=16)	
Hospital - length of stay (days) median (IQR)	29 (26)
PICU - length of stay (days) median (IQR)	12 (6.5)
Discharged to:	
Rehabilitation facility, n (%)	11 (48%)
Home, n (%)	5 (22%)

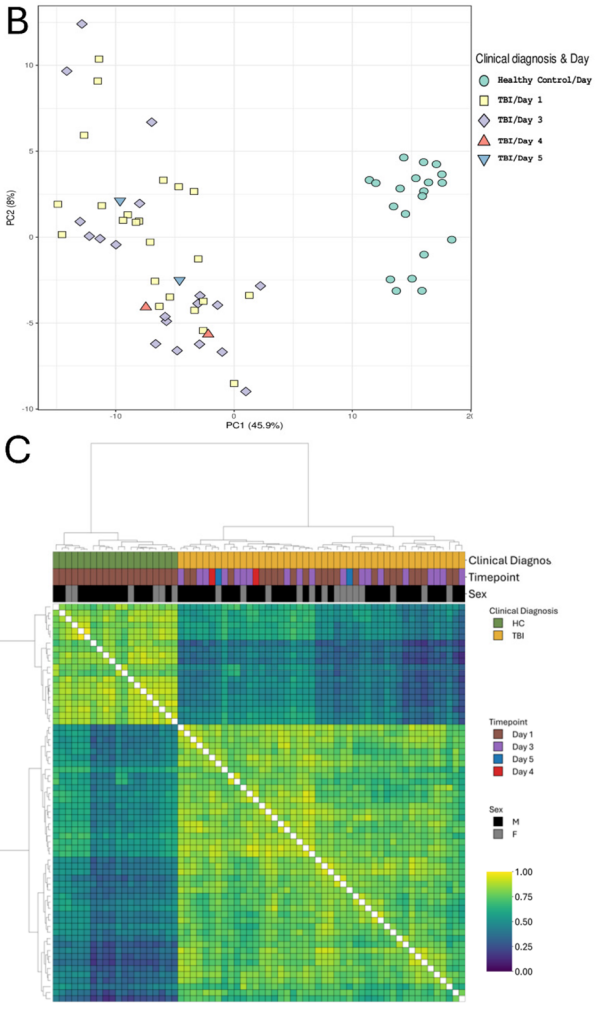


Fig. 1 Pediatric sTBI patient characteristics and plasma protein profiles quantified using the NULISAseq CNS Disease Panel. **A** Demographic and clinical data for pediatric sTBI patients. **B** An interactive scatterplot for the first principal components from the normalized data set. The colors in the plot correspond to one of the cohorts in the data set. **C** A heatmap showing the between-sample pairwise Pearson correlation of the normalized data. Individual samples are shown along both the X and Y axes, with the degree of correlation indicated by the color (yellow: higher correlation, purple: lower correlation). Clustering (Euclidean distance) is shown by the dendrograms above and to the left of the image, together with relevant annotation for each sample. Samples drawn on Day 3 ($n = 19$), Day 4 ($n = 2$) and Day 5 ($n = 2$) have a median number of days of 3 (IQR 0)

Canada). Plasma was isolated by centrifugation at 1,500 × g for 15 min at 4 °C (Brisson et al. 2012; Gillio-Meina et al. 2013); the upper plasma layer was aliquoted into 250-µL portions and immediately frozen at − 80 °C. Plasma samples underwent a single freeze–thaw cycle prior to analysis.

Conventional statistical analysis

Continuous demographic and clinical data are reported as medians with interquartile range (IQR) and are compared with healthy control subjects using Mann–Whitney U tests. Categorical variables are presented as n (%) and compared with healthy controls using Chi-square or Fisher's exact tests as appropriate. A one-way ANOVA with Benjamini–Hochberg FDR correction was used to compare mean protein expression between multiple groups.

Nucleic Acid Linked Immuno-Sandwich Assay (NULISA)

Plasma proteins were quantified using the NULISA-seq CNS Disease Panel, which measures 120 proteins across five neuropathologic domains: amyloid and tau pathology, synaptic and synuclein regulation, neurodegeneration, vascular and metabolic pathways, and neuroinflammation. Plasma samples were thawed, centrifuged at 10,000 × g for 10 min, and 10 µL of supernatant was transferred to 96-well plates for analysis.

NULISA uses paired antibodies specific to each protein target: (a) a capture antibody conjugated to partially double-stranded DNA with a poly-A tail and target-specific molecular identifier (TMI), and (b) a detection antibody conjugated to partially double-stranded DNA with a biotin group and corresponding TMI barcode, pooled in a multiplex panel. Upon incubation with samples, these antibodies form immunocomplexes with target proteins. Paramagnetic oligo-dT beads capture the complexes via dT-poly-A hybridization, and washing removes the sample matrix and unbound detection antibodies. Because dT-poly-A interactions are salt-sensitive, a low-salt buffer releases the immunocomplexes into solution. After bead removal, paramagnetic streptavidin-coated beads recapture the biotin-labeled immunocomplexes, and washing removes unbound capture antibodies. A ligation mix containing T4 DNA ligase, a DNA ligator sequence, and a sample-specific molecular identifier (SMI) joins proximal DNA ends on the antibody pair, generating a DNA reporter bearing unique TMI pairs and an SMI. Reporter abundance is quantified by next-generation sequencing on an Illumina NextSeq 2000 system.

Quality control and normalization

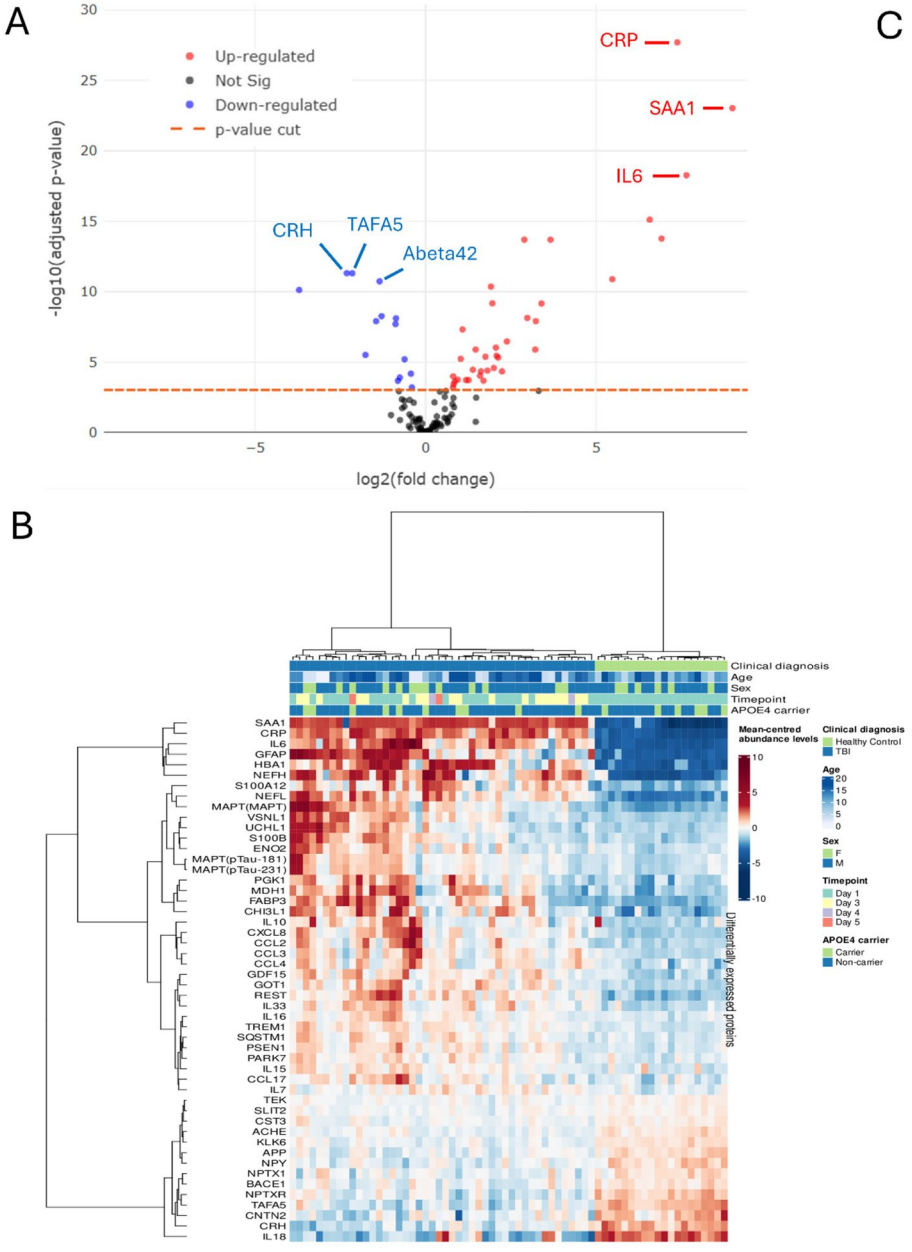
Proteomic data processing followed the standard NULISAseq pipeline (Feng et al. 2023). Raw sequencing count data were normalized through a two-step process to produce NULISA Protein Quantification (NPQ) units. First, intraplate normalization corrects for well-to-well variation by dividing each target's raw counts by the counts of an internal control protein (mCherry), a non-human protein spiked into every well. Second, the IC-normalized values are divided by the analyte-specific median counts from three interplate control (IPC) wells on the same plate. The resulting values are rescaled by a factor of 10^4, incremented by one, and $\log_2$-transformed to yield NPQ units, which are approximately normally distributed and suitable for standard downstream statistical analyses. Although no technical replicates were included, normalization using spiked-in internal controls and inter-plate reference wells minimized technical variability.

All 66 samples passed quality control and were retained for downstream analyses. Outliers were identified using four complementary metrics: sum of Euclidean distances to other samples, Kolmogorov–Smirnov test statistic, mean Pearson correlation with other samples, and Hoeffding's D statistic. Samples failing two or more criteria were flagged for exclusion; none met this threshold. Data were visually inspected using kernel density plots and PCA plots. All 120 protein targets met detectability thresholds and were retained. sTBI and control samples were randomized across a single plate, and normalization against spiked-in and inter-plate controls effectively minimized plate- and run-level technical effects.

To assess potential confounding, we examined pairwise associations among all clinical covariates. After FDR correction, only the age-weight, PICU length of stay, and hospital length of stay associations remained significant, indicating that key injury severity variables were largely independent of one another and reducing the likelihood that any single clinical factor systematically drove the observed proteomic signal (Supplemental Fig. 2).

Differential expression analysis

Differences in normalized protein expression values ($\log_2$ transformed) between sTBI patients (PICU Day 1 and Day 3) and healthy controls were assessed using empirical Bayes moderated t-tests implemented in the limma R package (healthy controls vs sTBI PICU Day 1 (Fig. 2); sTBI PICU Day 3 vs sTBI PICU Day 1 (Fig. 3)). For longitudinal comparisons between PICU Day 1 and Day 3, a paired analysis was performed by including subject (patient ID) as a factor in the linear model to account for within-subject variability, thereby estimating changes within individuals. To account for multiple testing, p-values were adjusted using the false discovery rate (FDR). Positive $\log_2$ fold changes indicated increase, and negative $\log_2$ fold changes indicated decrease. Proteins exhibiting an FDR-adjusted $p < 0.05$ were considered differentially expressed.

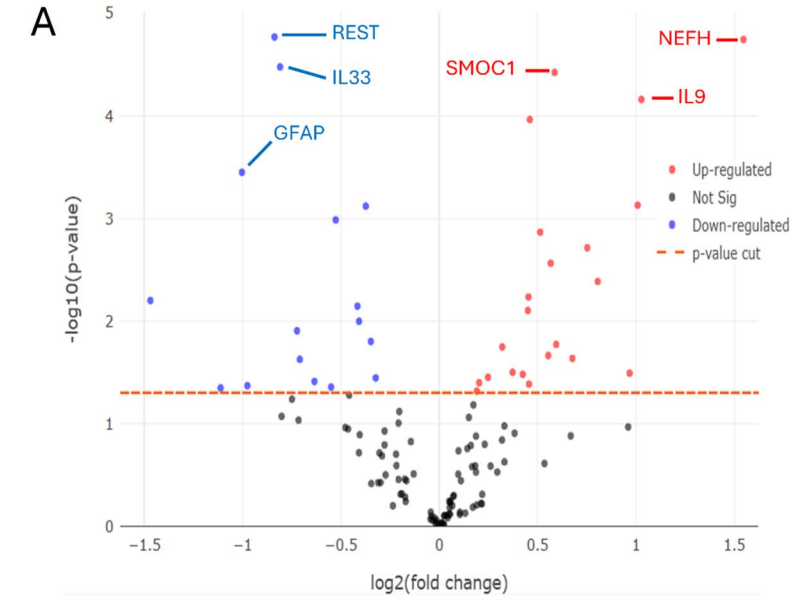


C

Protein	Fold Change	adj.P.val
CRP	165.553	1.97E-28
SAA1	507.414	9.31E-24
IL6	199.237	5.42E-19
HBA1	94.579	7.93E-16
GFAP	120.237	1.73E-14
NEFL	12.59	2.07E-14
REST	7.406	2.07E-14
CRH	-4.976	5.04E-12
TAFA5	-4.451	5.10E-12
NEFH	44.249	1.34E-11
Abeta42	-2.557	1.90E-11
IL33	3.751	4.56E-11
IL18	-13.095	7.92E-11
GOT1	3.863	7.02E-10
FABP3	10.489	7.27E-10
NPY	-2.458	5.66E-09
MDH1	7.869	7.54E-09
ACHE	-1.831	8.14E-09
CHI3L1	9.347	1.29E-08
NPTXR	-2.745	1.29E-08
KLK6	-1.852	2.07E-08
TREM1	2.106	4.99E-08
VSNL1	5.194	3.57E-07
S100A12	4.156	9.79E-07
GDF15	2.751	1.34E-06
MAPT	9.234	1.34E-06
CNTN2	-3.412	3.25E-06
CXCL8	4.205	3.74E-06
ENO2	3.361	4.36E-06
PGK1	4.343	5.02E-06
IL16	2.031	6.20E-06
CST3	-1.54	6.63E-06
S100B	3.973	2.78E-05
CCL4	2.599	3.71E-05
IL10	3.495	4.18E-05
UCHL1	4.706	4.81E-05
pTau-231	3.067	4.81E-05
SLIT2	-1.355	7.03E-05
pTau-181	3.01	9.80E-05
IL7	1.743	0.000107

Fig. 2 Association tests between sTBI PICU Day 1 patients and healthy controls shown graphically and with a ranking of significant DEPs. **A** Volcano plot showing statistical significance (−log10 FDR-adjusted p-value) against magnitude of change (log2 fold change, signed) for all 120 proteins quantified. Increased proteins are shown in red, decreased proteins in blue, and non-significant proteins in black. A negative log2 fold change indicates decreased abundance in sTBI relative to healthy controls. The horizontal orange line represents the FDR-adjusted p-value threshold. **B** Heatmap showing protein intensity per sample relative to the mean level across DEPs; individual proteins are shown on the y-axis and samples on the x-axis, with red and blue cells indicating higher and lower relative protein levels, respectively. **C** Table listing the top 40 DEPs ranked by FDR-adjusted p-value, reporting both signed log2 fold change and linear fold change (ratio); red text indicates increased and blue text indicates decreased plasma proteins in sTBI patients relative to healthy controls

For temporal comparisons (Fig. 4), an ANOVA framework was applied to assess changes across all three groups (healthy controls, sTBI PICU Day 1, sTBI PICU Day 3). Multiplicity control was applied consistently across both approaches using Benjamini–Hochberg FDR correction. Critically, all proteins identified as significant in the temporal analyses were also significant under the limma paired modeling approach, confirming consistency across methods. The ANOVA framework was retained for Fig. 4 to facilitate a visually intuitive three-way comparison.



C

Protein	Fold Change	adj.P.val
REST	-1.788	0.00111
NEFH	2.92	0.00111
IL33	-1.753	0.00116
SMOC1	1.501	0.00116
IL9	2.038	0.00171
MSLN	1.375	0.00223
GFAP	-2.005	0.00625
S100A12	2.011	0.0104
POSTN	-1.296	0.0104
pTau-231	-1.441	0.0127
TREM2	1.427	0.0152
NEFL	1.684	0.0198
IL12p70	1.48	0.0259
CCL13	1.747	0.0362
NGF	1.369	0.0477
MDH1	-2.768	0.0484

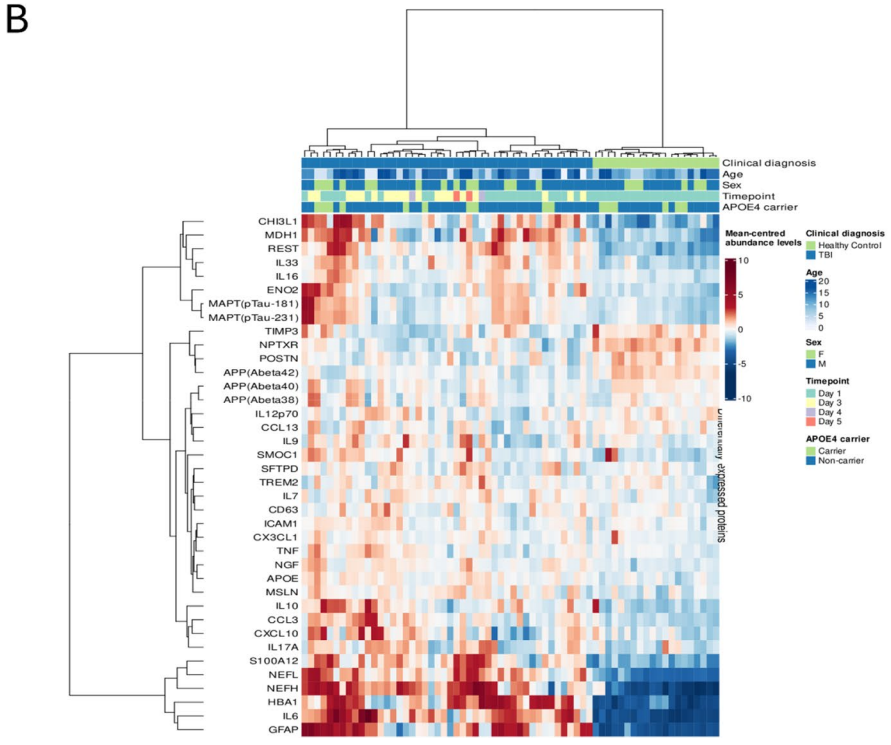


Fig. 3 Association tests between sTBI PICU Day 3 and Day 1 patients shown graphically and with a ranking of significant DEPs. **A** Volcano plot showing statistical significance (− log10 FDR-adjusted p-value) against magnitude of change (log2 fold change, signed) for all 120 proteins quantified. Increased proteins are shown in red, decreased proteins in blue, and non-significant proteins in black. A negative log2 fold change indicates decreased abundance in sTBI PICU Day 3 relative to Day 1 patients. The horizontal orange line represents the FDR-adjusted p-value threshold. **B** Heatmap showing protein intensity per sample relative to the mean level across DEPs; individual proteins are shown on the y-axis and samples on the x-axis, with red and blue cells indicating higher and lower relative protein levels, respectively. **C** Table listing all 16 DEPs ranked by FDR-adjusted *p*-value, reporting both signed log2 fold change and linear fold change (ratio); red text indicates increased and blue text indicates decreased plasma proteins in sTBI PICU Day 3 relative to Day 1 patients

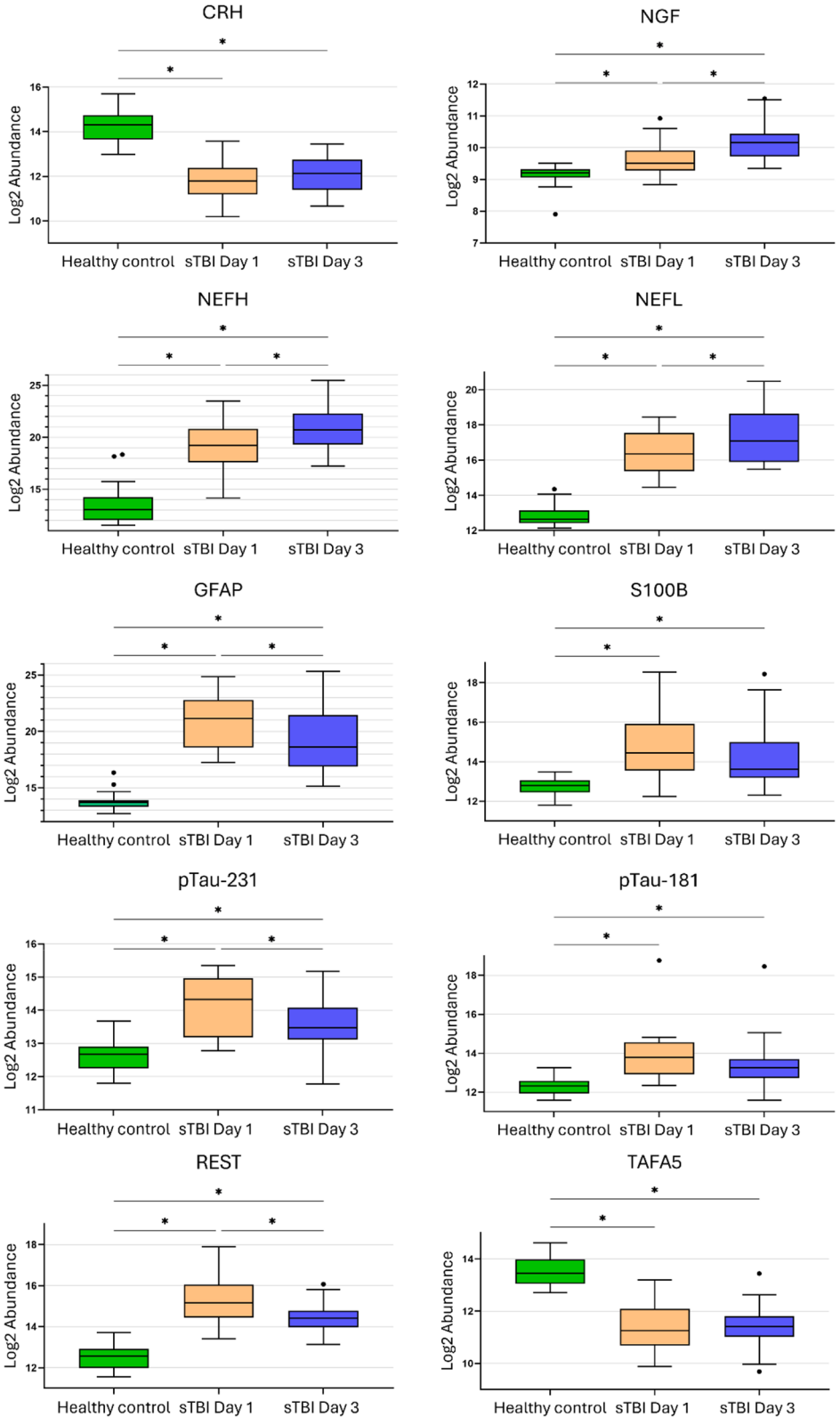


Fig. 4 Box Plots illustrating the log2 abundance levels of brain-associated proteins across three groups: Healthy Controls, sTBI PICU Day 1, and sTBI PICU Day 3. The proteins analyzed include neuropeptides (CRH and NGF), neuron-specific filament proteins (NEFH and NEFL), astrocyte-specific proteins (GFAP and S100B), phosphorylated Tau proteins (pTau-231 and pTau-181), and brain proteins involved in cellular regulation and signaling (REST and TAFA5). The horizontal line below the asterisks indicates the groups that have a significant difference in terms of median in the expression of proteins

Protein-clinical variable association analysis

Clinical metadata were cleaned and preprocessed prior to analysis. Features with missing values or zero variance were excluded and manually identified irrelevant features were removed. Categorical features were encoded using one-hot encoding to enable correlation analyses with continuous protein biomarker levels. For binary variables (indicating presence or absence of a given injury), the one-hot encoding process created two features: one for presence and one for absence. Only the 'positive/present' category was used in subsequent analyses to avoid redundancy. For categorical variables with more than two categories, separate binary features were created for each category. Correlations were calculated between continuous protein biomarker levels and clinical variables to assess associations between protein expression and clinical features. For each comparison, Pearson correlation coefficients and associated p-values were computed. The corresponding p-values were used to mask the correlation coefficients: only significant correlations (FDR-adjusted $p < 0.05$) are displayed in figures.

Protein–protein interactions

PPI analysis was performed to identify functional relationships and pathways among differentially expressed proteins (DEPs) in pediatric sTBI. Proteins meeting the significance threshold (FDR-adjusted $p \leq 0.05$) from the comparison of sTBI PICU Day 1 versus healthy controls were used for network analysis. PPI networks were constructed using STRING, which integrates known and predicted protein interactions from experimental data, curated databases, co-expression, gene neighborhood, gene fusion, and text mining. Only experimentally supported and database-curated interactions were included, with a minimum interaction confidence score of 0.7 (high). Networks were restricted to first-shell interactions to preserve interpretability and avoid overexpansion. Proteins were mapped using official gene symbols, and disconnected nodes were excluded. Functional clustering was performed using k-means clustering ($k = 5$), where k was selected to aid biological interpretability.

Functional enrichment: cellular and tissue

Tissue and cellular compartment enrichment were assessed using the integrated TISSUES database to identify anatomical and cellular localization patterns. Enrichment significance was evaluated using hypergeometric testing with Benjamini–Hochberg correction, and terms with FDR-adjusted $p < 0.05$ were considered significant. The node size reflected degree of connectivity, and the signal strength and line color intensity indicated the interaction confidence. Clusters were interpreted based on dominant enriched terms and known functional roles of constituent proteins.

Results

Patient demographic and clinical data

We examined the plasma proteomes of 23 participants with sTBI and 20 age- and sex-matched healthy controls. Participant demographic and clinical data are provided in Fig. 1A. The sTBI cohort had a median age of 15 years (IQR 10) and was 70% male ($n = 16$). Motor vehicle collisions were the cause of 70% ($n = 16$) of injuries. The median injury severity score (ISS) was 33 (IQR 9), with a median pre-sedation GCS score of 4 (IQR 2). Principal component analysis of normalized proteomic data demonstrated distinct clustering between groups, with healthy controls showing tighter grouping and sTBI patients exhibiting greater variability (Fig. 1B). Correlation heatmap analysis confirmed higher within-group similarity among healthy controls compared to sTBI patients (Fig. 1C).

Differentially expressed proteins

Comparison of sTBI PICU Day 1 versus healthy controls plasma samples identified 67 DEPs at FDR-adjusted $p < 0.05$: 46 increased and 21 decreased (Fig. 2). A complete list of the 67 DEPs and their neurobiological classification is shown in Supplemental Table 1. Volcano plot analysis (Fig. 2A) displays the magnitude and significance of protein changes, with increased (red dots) and decreased (blue dots) proteins. Hierarchical clustering heatmap analysis (Fig. 2B) reveals distinct protein abundance patterns between sTBI patients and healthy controls, with clear separation of the two cohorts. The top 40 DEPs ranked by statistical significance are presented in Fig. 2C.

Within our panel, 10 of 31 synaptic function proteins, 8 of 15 amyloid/tau pathology proteins, and 31 of 51 inflammatory mediators reached significance. The most increased proteins were Serum amyloid A1 (SAA1; fold change [FC] 507.414), Interleukin-6 (IL-6; FC 199.237), and C-reactive protein (CRP; FC 165.553). Additional increased interleukins included IL-33, IL-16, IL-10, and IL-7. Chemokine ligands CXCL8 and CCL4 were also increased. The most decreased proteins were Corticotropin-releasing hormone (CRH; FC −4.976), TAFA chemokine like family member 5 (TAFA5; FC −4.451), and Amyloid beta 42 (Aβ42; FC −2.557). Additional decreased proteins included IL-18, Neuropeptide Y (NPY), Acetylcholinesterase (ACHE), Neuronal pentraxin receptor (NPTXR), Kallikrein related peptidase 6 (KLK6), Contactin-2 (CNTN2), Cystatin C (CST3), and Slit guidance ligand 2 (SLIT2).

Comparison of sTBI PICU Day 3 versus PICU Day 1 identified 16 DEPs: 10 increased and 6 decreased (Fig. 3). Volcano plot visualization (Fig. 3A) demonstrates temporal changes in protein abundance between PICU Day 1 and PICU Day 3 samples, showing a smaller number of

DEPs compared to the PICU Day 1 versus healthy controls comparison. All 16 statistically significant proteins with their fold changes and adjusted p-values are listed in Fig. 3C. Increased proteins on PICU Day 3 relative to PICU Day 1 included neurofilament heavy chain (NEFH), SPARC related modular calcium binding 1 (SMOC1), IL9, Mesothelin (MSLN), S100 calcium binding protein A12 (S100A12), Triggering receptor expressed on myeloid cells 2 (TREM2), Neurofilament light chain (NEFL), IL12p70, CCL13, and Nerve growth factor (NGF). Decreased proteins on PICU Day 3 relative to PICU Day 1 included RE1-silencing transcription factor (REST), IL33, Glial fibrillary acidic protein (GFAP), Periostin (POSTN), phosphorylated tau-231 (pTau-231), and Malate dehydrogenase 1 (MDH1). Comprehensive statistical analysis results for all proteins are provided in Supplemental Tables 2 and 3.

Temporal patterns of brain-specific proteins

Brain-specific proteins showed differential expression (Fig. 4) across all three comparisons (healthy controls vs. sTBI PICU Day 1 vs. sTBI PICU Day 3). Three proteins demonstrated sustained elevation: NGF, NEFH, and NEFL showed progressive increases from controls through PICU Day 1 to PICU Day 3. Seven proteins exhibited biphasic temporal patterns (Fig. 4). Five proteins (GFAP, S100B, pTau-231, pTau-181, and REST) showed initial increases at PICU Day 1 followed by declines at Day 3. Conversely, two proteins (CRH and TAFA5) demonstrated the opposite trajectory, with initial suppression at Day 1 followed by recovery at Day 3.

Protein–protein interactions

STRING network analysis of the 67 DEPs from sTBI PICU Day 1 compared with controls reveals a highly interconnected network with distinct functional clusters (Fig. 5). K-means clustering identified two dominant clusters and three smaller clusters. The largest functional cluster consists of proteins involved in leukocyte chemotaxis and cytokine-cytokine receptor interactions, such as CRP, SAA1, IL-6, IL-10, IL1B, IL18, IL33, IL7, IL16, multiple CCLs, CXCL8, TREM1, and S100A12. This cluster included both pro- and anti-inflammatory cytokines. The second major cluster includes proteins involved in amyloid precursor protein metabolism, comprising Amyloid precursor protein (APP), Beta-site APP-cleaving enzyme 1 (BACE1), Presenilin-1 (PSEN1), Microtubule-associated protein tau (MAPT), Apolipoprotein E (APOE), GFAP, NEFL, and NEFH. The neuropeptide hormone activity cluster contains CRH and NPY; the peroxiredoxin activity/Parkinson disease cluster contains Ubiquitin C-terminal hydrolase-L1 (UCHL1), Parkinsonism associated deglycase (PARK7), and Peroxiredoxin-6 (PRDX6); and the VEGF ligand-receptor interactions and Tie signaling pathway cluster contains TEK receptor tyrosine kinase (TEK) and Vascular endothelial growth factor (VEGF-D). IL-6 occupied a bridging position in the network, connecting the large inflammatory cluster with brain-specific protein clusters, including the amyloid metabolism cluster and smaller functional groups.

Cellular component and tissue expression enrichment

Gene Ontology cellular component analysis identified significant enrichment in multiple categories (Fig. 6A). Neuronal-specific terms included neuronal cell body, somatodendritic compartment, axon, and synaptic cleft. Structural terms included membrane raft and postsynaptic intermediate filament cytoskeleton. The most enriched term was extracellular space/extracellular region. TISSUES database enrichment analysis identified significant protein localization patterns across distinct tissue and pathological categories (Fig. 6B). Pathological features showed enrichment in amyloid plaques and neurofibrillary tangles. Brain regions with significant enrichment included entorhinal cortex and parietal/occipital lobes. Cellular enrichment analysis demonstrated significant representation in microglia, granulocytes, neutrophils, and phagocytes, with granulocytes exhibiting the strongest enrichment among immune cell populations.

Protein-clinical variable correlation analysis: sTBI PICU day 1 versus healthy controls

Pearson correlation analysis between DEPs and clinical/demographic variables on PICU Day 1 (compared to healthy controls) revealed several significant associations (Fig. 7; Suppl. Table 4). Age showed positive correlations with ACHE and membrane metalloendopeptidase (MME), and negative correlations with BACE1 and NPTXR. Serum sodium levels demonstrated several positive correlations, most notably with Enolase 2 (ENO2), MAPT, and phosphorylated tau (pTau) isoforms pTau-181, pTau-217, and pTau-231. MAPT additionally correlated with both brain herniation and mortality. Mortality was associated with elevated expression of multiple inflammatory markers, including CCL2, CCL3, and CCL4. ISS showed several positive correlations, most notably with REST and IL-16. However, correlations pertaining to mortality and other outcomes are not significant when considering FDR-corrected significance.

Skull fracture location exhibited distinct protein expression patterns. Vault fractures demonstrated predominantly negative correlations, most notably with Sequestosome 1 (SQSTM1), PSEN1, and IL-16, whereas basal skull fractures showed a strong positive correlation with POSTN. VEGF-D was the only protein negatively correlated with death and was positively associated with discharge to a rehabilitation facility. Frequencies for clinical variable values are presented in Supplemental Fig. 3.

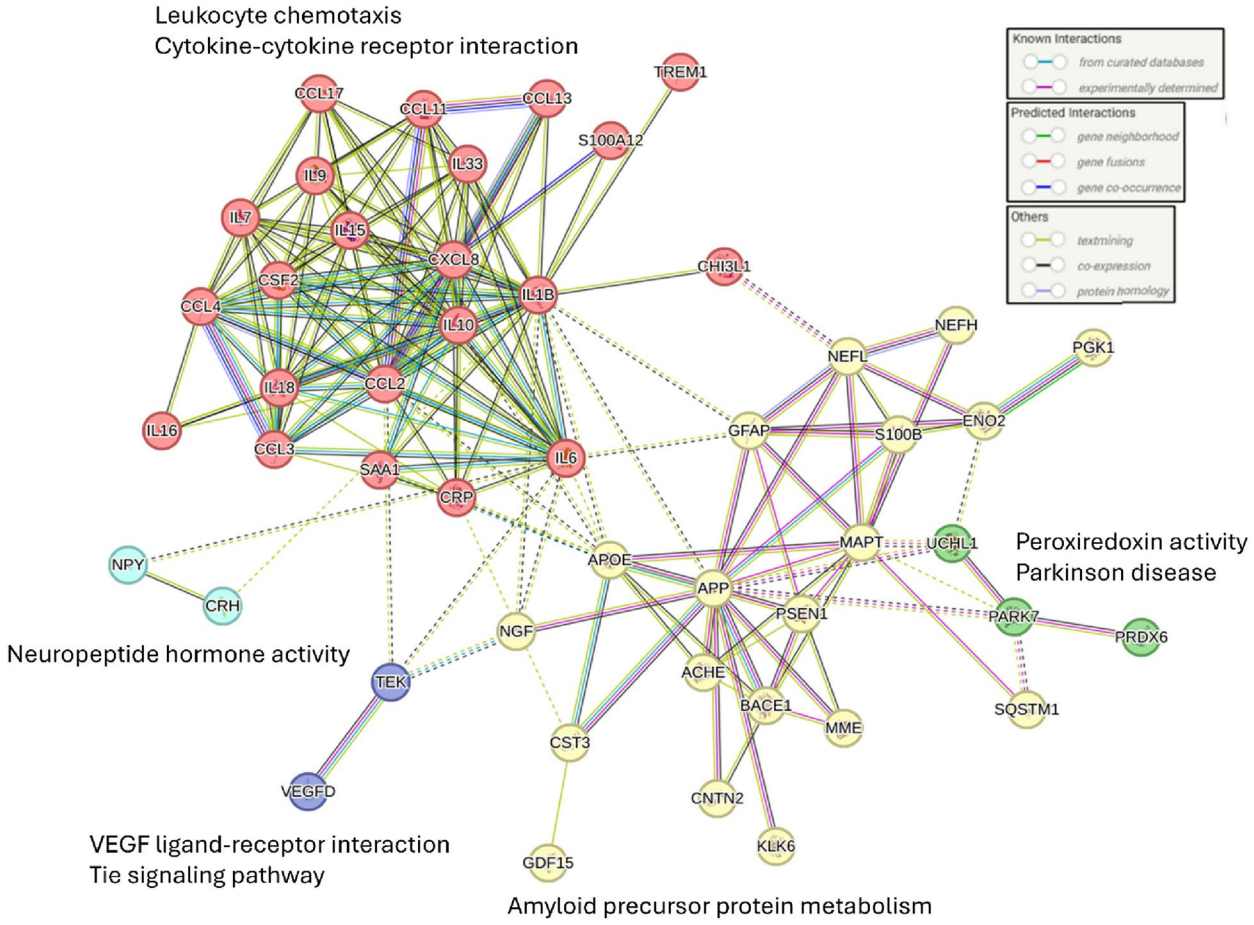


Fig. 5 STRING database PPI network of DEPs in pediatric sTBI. STRING analysis of significantly dysregulated proteins identified through proteomic profiling shows a highly interconnected network with functional clustering. Nodes represent individual proteins, with node colors indicating different functional groups. Edges represent PPIs with different line types and colors indicating the source of interaction evidence as shown in the legend. The minimum interaction was set at 0.7 (high confidence). The network reveals several distinct functional clusters including a large inflammatory response cluster centered around cytokines and chemokines (CRP, SAA1, IL-6, etc.) that is associated with "Leukocyte chemotaxis" and "Cytokine-cytokine receptor interaction" pathways. Another large cluster comprised of proteins in yellow (GFAP, NEFL, NEFH, etc.) is "amyloid precursor protein metabolism". Smaller brain-associated clusters include proteins involved in "Neuropeptide hormone activity" (CRH, NPY), "Peroxiredoxin activity/Parkinson disease" (UCHL1, PARK7, PRDX6), and "VEGF ligand-receptor interactions and Tie signaling pathway" (TEK, VEGFD). IL-6 appears to bridge inflammatory and neurological specific clusters, suggesting interaction between inflammatory/immune processes and brain-specific pathways in pediatric sTBI

Protein-clinical variable correlation analysis: sTBI PICU Day 3 Versus sTBI PICU Day 1

Correlation analysis comparing sTBI patients on PICU Day 3 versus PICU Day 1 (Fig. 8; Suppl. Table 5) revealed both persistent and evolving protein-clinical variable associations relative to those observed at PICU Day 1 versus healthy controls. Serum sodium continued to show positive correlations with pTau-231, GFAP, NEFL, NGF, and a timepoint-specific correlation with SMOC1. ISS remained positively correlated with REST.

S100A12 remained negatively correlated with both vault skull fractures and epidural hemorrhage, whereas POSTN showed persistent strong positive correlation with basal skull fractures. Secondary brain injury markers demonstrated notable associations at this timepoint. pTau-231 remained positively correlated with brain herniation. Conversely, herniation showed negative correlation with TREM2, while GFAP was positively associated with mortality.

A notable shift in clinical correlations occurred between timepoints: IL-12p70 maintained positive correlation with platelet count, while only SMOC1 and IL-12p70 correlated with GCS at PICU Day 3, representing a substantial reduction from the multiple GCS-associated proteins observed on PICU Day 1.

Discussion

This exploratory study represents the most comprehensive neuro-proteomic assessment of pediatric sTBI reported to date, quantifying changes in proteins annotated to neurodegeneration, synaptic biology, vascular dysfunction, metabolism, and inflammation. By profiling

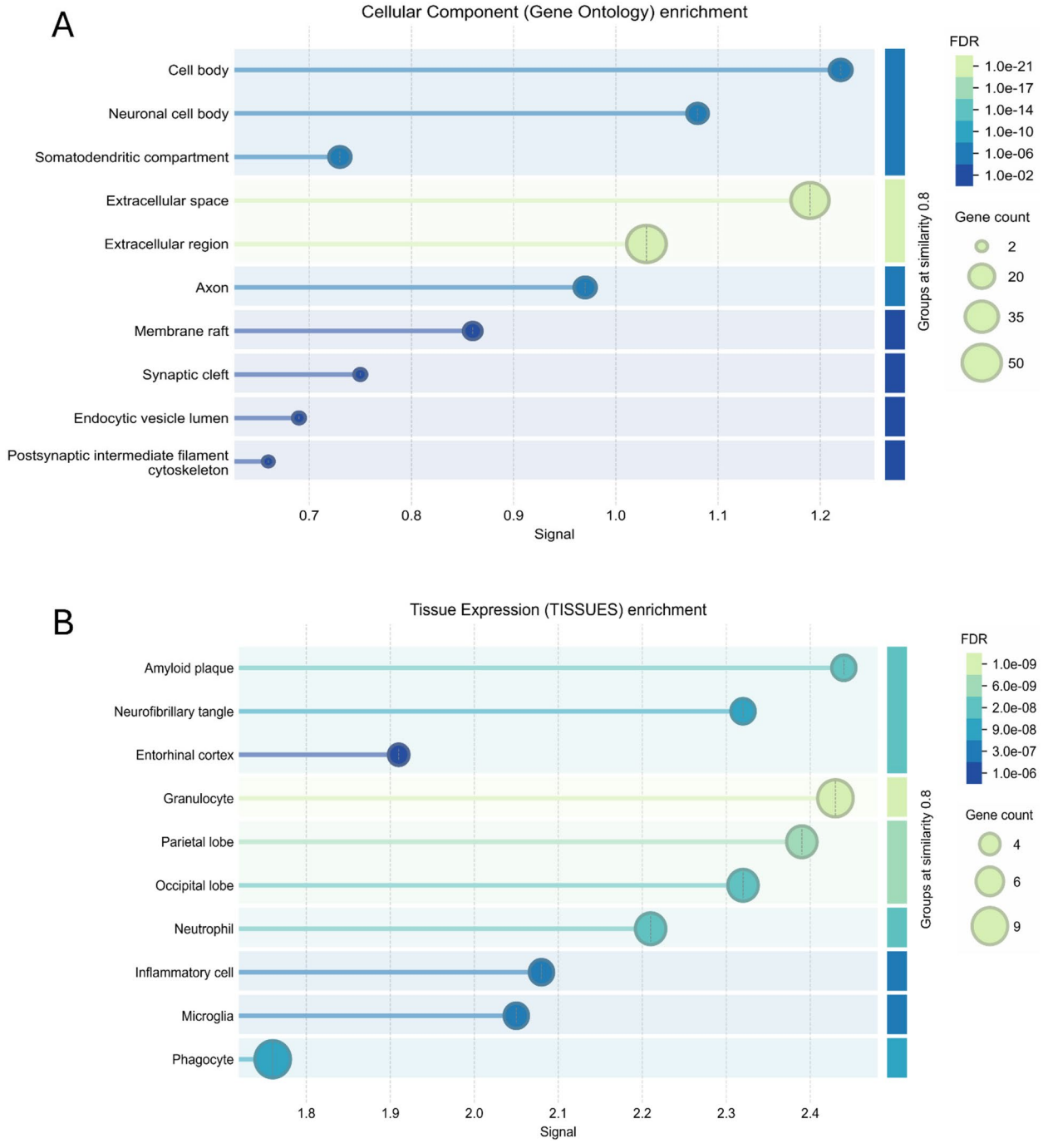


Fig. 6 Cellular component and tissue expression analysis of the pediatric sTBI proteome (sTBI PICU Day 1 vs Healthy Controls): **A** Gene Ontology (GO) cellular component enrichment analysis of 67 DEPs identified from the sTBI PICU Day 1 vs. healthy controls contrast, performed using the STRING database (v12.0) with the Homo sapiens background proteome and FDR-corrected p-values as the significance threshold. Enriched terms reflect the known subcellular compartment annotations of the identified proteins, with top categories including extracellular space/region, neuronal cell body, somatodendritic compartment, axon, and synaptic cleft. **B** TISSUES 2.0 database enrichment analysis of the same 67 DEPs, using the integrated tissue expression and disease annotation corpus with FDR correction. Panels **A** and **B** were performed independently using mutually exclusive databases, applied to the same input DEP list. All enrichment results reflect the known prior annotations and tissue expression profiles of the identified proteins, not direct in vivo neuropathological findings inferred from plasma measurement alone. The x-axis represents enrichment score (signal strength), bubble size indicates gene count, and colour intensity represents FDR value, with lighter colours indicating lower (more significant) FDR

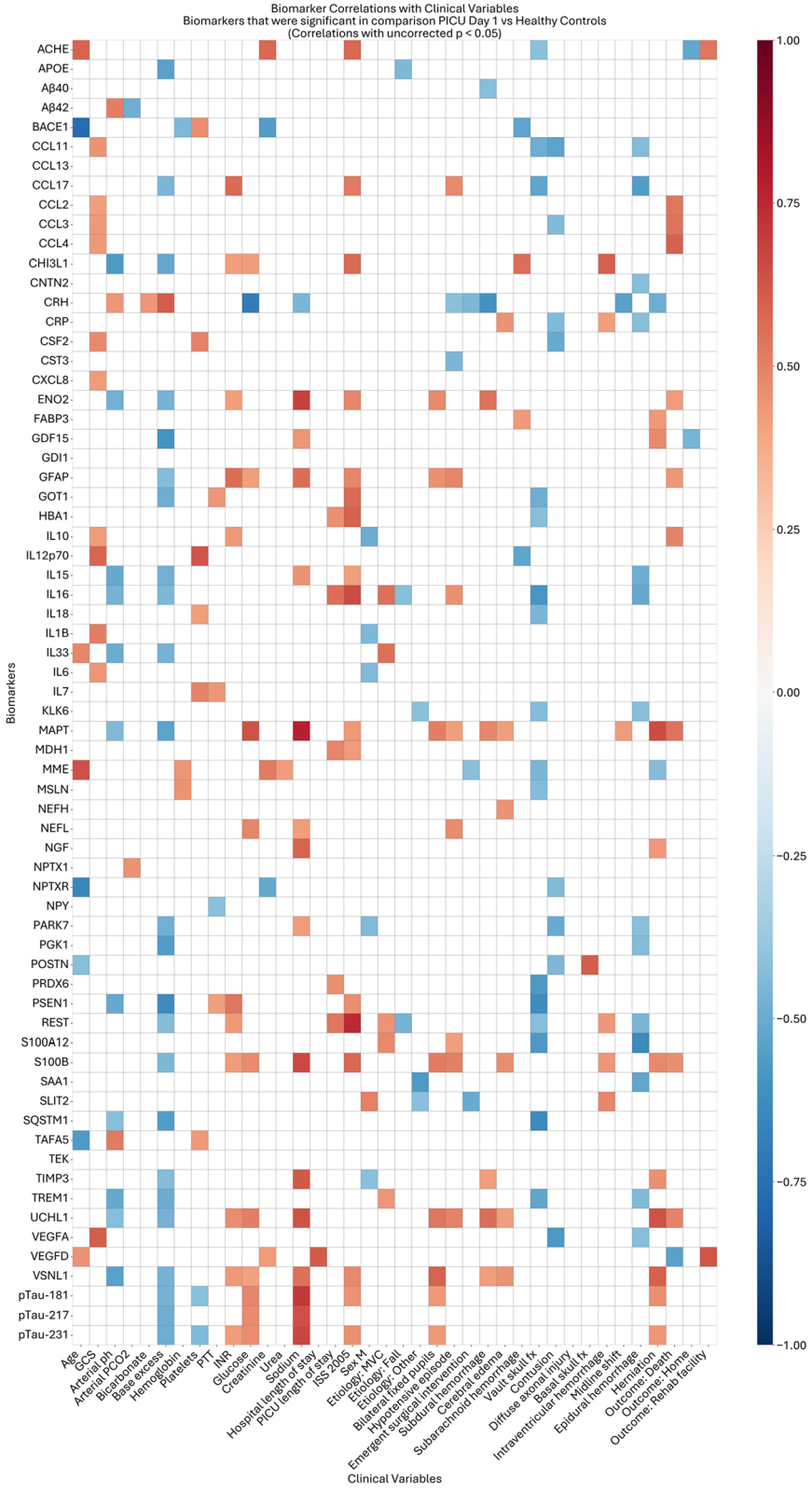


Fig. 7 Associations Between Differential Protein Expression (sTBI PICU Day 1 Versus Healthy Controls) and Clinical Variables. Heatmap illustrating significant correlations between DEPs and clinical outcomes. Color represents direction of association: red for positive correlations and blue for negative correlations. Color intensity correlates to strength of association. Only significant correlations are displayed, defined as those with adj. $p < 0.05$

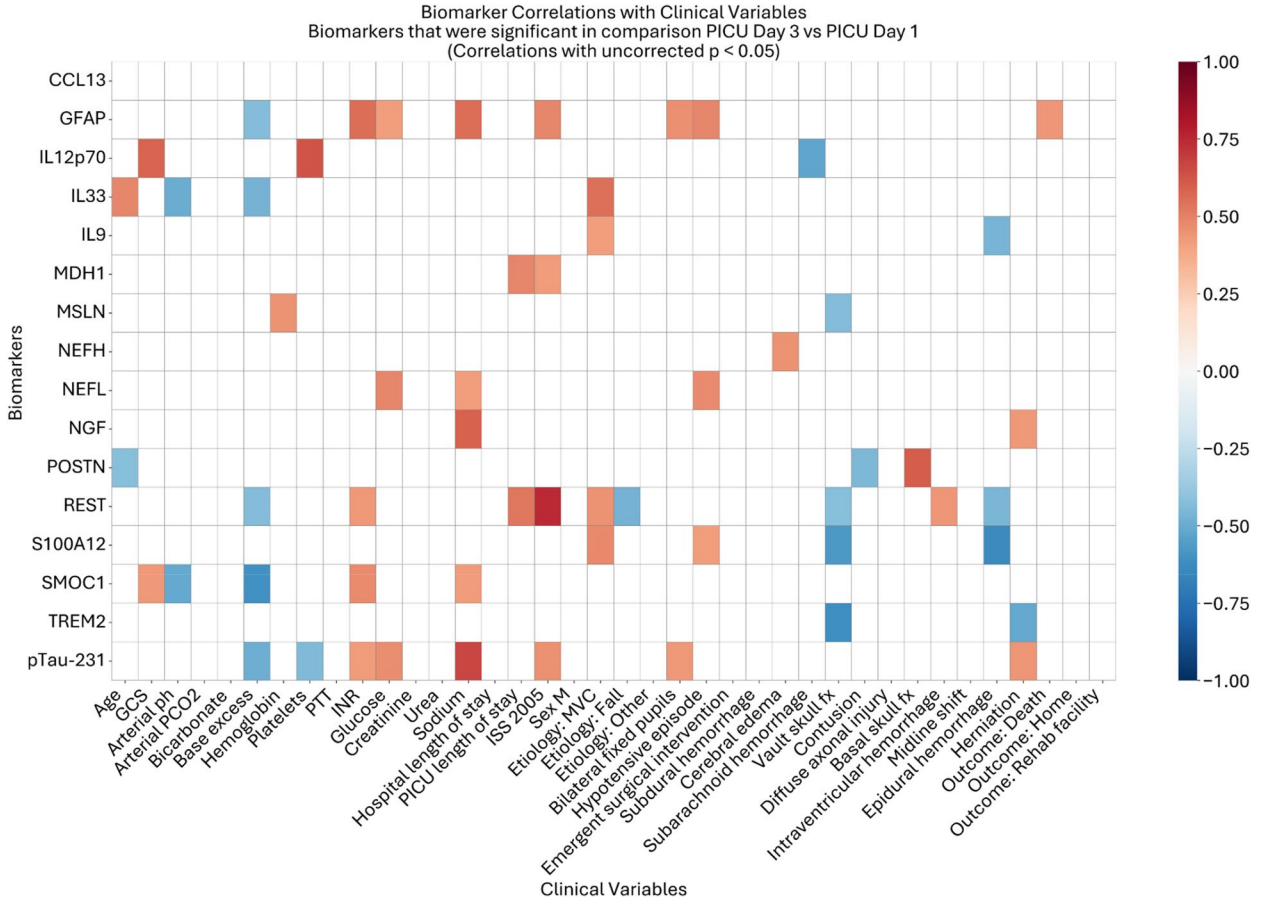


Fig. 8 Associations Between Differential Protein Expression (sTBI PICU Day 3 Versus sTBI PICU Day 1) and Clinical Variables. Heatmap illustrating significant correlations between DEPs and clinical outcomes. Color represents direction of association: red for positive correlations and blue for negative correlations. Color intensity correlates to strength of association. Only significant correlations are displayed, defined as those with adj. $p < 0.05$

120 proteins across five distinct neuropathologic domains during the acute phase of injury, we identified 67 DEPs at PICU admission on Day 1 and captured their temporal evolution through PICU Day 3. These findings suggest a complex interplay between neuroinflammatory cascades and neurodegenerative processes, with several brain-specific proteins demonstrating distinct temporal trajectories. PPI network analysis suggests pathways centered on APP metabolism and cytokine-mediated inflammation, with IL-6 emerging as a critical hub linking these domains.

The demographic and clinical characteristics of our cohort are consistent with those of established pediatric sTBI populations. Indeed, the age and sex distributions align with prior cohorts (Daley et al. 2022; Kolsto et al. 2025; Marzano et al. 2022). The median ISS and presedation GCS score are also comparable to other multicenter pediatric sTBI studies (Bell et al. 2013; Kochanek et al. 2019), confirming injury severity. Motor vehicle collisions accounted for most injuries, consistent with traffic-related incidents representing the leading mechanism of pediatric sTBI (Dewan et al. 2016; Abeytunge et al. 2021; Haydel et al. 2025). The MAIS head and PICU admission further corroborate injury severity (Dewan et al. 2016; Riemann et al. 2020).

Although biological heterogeneity in TBI is increasingly recognized (Maas et al. 2022; Tenovuo et al. 2021), molecular endotyping studies in pediatric populations remain limited. While adult TBI research has advanced through large-scale initiatives like CENTER-TBI, which identified endotypes distinguished by neurological presentation and metabolic profiles (Åkerlund et al. 2024; Stocchetti et al. 2017), pediatric-specific investigations have been constrained by predominantly single-analyte approaches. Early proteomic profiling in pediatric sTBI demonstrated 95 DEPs, suggesting peripheral proteomic signatures can reflect sTBI biology (Haqqani et al. 2007). A recent multi-omics study reported the first integrated transcriptomic and metabolomic analysis in pediatric sTBI, revealing dysregulated immune pathways and metabolic perturbations (Hussain et al. 2025). However, proteomics-based endotyping in pediatric populations has focused primarily on established brain biomarkers such as GFAP, S100B, NSE, and neurofilament proteins

(Fraser et al. 2011; Marzano et al. 2022; Chiaretti et al. 2008; Žurek and Fedora 2012), without broad proteomic coverage or systems-level analysis. Our study aims to generate preliminary insights into the molecular signatures that may underlie heterogeneous outcomes in pediatric sTBI, leveraging high-dimensional proteomics as an exploratory tool to identify candidate proteins and pathways warranting investigation in larger, outcome-stratified cohorts.

The distribution of DEPs belonged to five neuropathologic domains, with inflammation as the predominant molecular signature (31/51 DEPs). This aligns with established understanding of pediatric TBI pathophysiology, wherein neuroinflammation drives secondary injury through blood–brain barrier disruption, peripheral immune cell recruitment, and microglial activation (Serpa et al. 2021; Riemann et al. 2020; McKee and Lukens 2016). This robust inflammatory response is consistent with recent transcriptomic and metabolomic studies demonstrating widespread immune pathway dysregulation (Hussain et al. 2025).

The co-expression of DEPs across amyloid and tau pathologies (8/15 DEPs) and synaptic regulation (10/31 DEPs) underscores the multi-system nature of pediatric sTBI (Maas et al. 2022). Emerging evidence suggests pediatric sTBI may exhibit a uniform inflammatory endotype characterized by robust cytokine elevation during the acute phase (Ryan et al. 2022; Huang et al. 2024; Samanta et al. 2024), accompanied by concurrent activation of neurodegenerative cascades, including amyloid-β and hyperphosphorylated tau accumulation (Johnson et al. 2010; Edwards et al. 2020). This pattern may reflect unique features of the developing brain, including heightened neuroinflammatory responses, ongoing myelination, and increased vulnerability to excitotoxicity and oxidative stress (Serpa et al. 2021; Walker et al. 2009; Figaji 2017). The simultaneous disruption across multiple neuropathologic domains provides a molecular basis for the clinical heterogeneity observed in pediatric TBI outcomes and supports the hypothesis that effective therapeutic strategies will require multi-targeted, pathway-informed approaches.

The acute inflammatory signature in our cohort was characterized by coordinated increase of pro-inflammatory mediators (IL-6, IL-33, IL-16, IL-7) balanced by anti-inflammatory responses (increased IL-10, decreased IL-18). IL-33 functions as an alarmin that activates immune cells following trauma (Erenler and Baydin 2020; Miller 2011), propagating responses through cytokines that induce leukocyte chemotaxis and microglial activation (Chen et al. 2021; Niewold et al. 2025; Caceres et al. 2025). The chemokine ligands CXCL8 and CCL4 further amplify this inflammatory cascade (Semple et al. 2010), while increased IL-10 represents concurrent resolution mechanisms (Garcia et al. 2017). We also identified dysregulation of markers less commonly reported in pediatric TBI, including synaptic regulatory proteins (NPTX1, NPTXR, CNTN2) and vascular integrity mediators (TEK/TIE2, VEGF-A, VEGF-D), which may represent overlooked contributors to long-term neurodevelopmental outcomes (Xanthos and Sandkühler 2014; Jullienne et al. 2016). The relatively higher protein abundance observed in the healthy control cluster within Fig. 2B reflects proteins that are significantly decreased in sTBI patients compared to controls, including neuropeptides (CRH, NPY), synaptic regulators (NPTXR, ACHE), and amyloid-associated proteins (APP, Aβ42). These proteins represent a biologically coherent set of CNS-homeostatic mediators whose suppression following sTBI is consistent with acute neurological injury disrupting normal synaptic and neuropeptide signaling.

By PICU Day 3, the proteomic landscape demonstrates relative suppression of the acute inflammatory response compared to PICU Day 1, despite evidence of persistent immune activation. Decreased IL-33 suggests reduced inflammatory maintenance (Erenler and Baydin 2020), while TREM2 elevation, a microglial receptor that promotes anti-inflammatory gene expression (Liu et al. 2020; Zhang and Chen 2023), may suggest a phenotypic transition. Increased IL-9 and IL-12p70 (Hamza et al. 2010; Lassaren et al. 2021) demonstrated ongoing but modulated immune responses, consistent with secondary injury evolution. STRING network analysis positioned IL-6 as a central hub connecting inflammatory and neurodegenerative cascades, suggesting coordinated immune activation and neural injury. This network encompassed acute-phase reactants (CRP, SAA1) that propagate neuroinflammation through cytokine amplification (Farre-Alins et al. 2021; Wang et al. 2025), chemokines mediating immune cell recruitment (Gyoneva and Ransohoff 2015), and surface receptors/ligands (TREM1, S100A12) enhancing leukocyte activation (Feng et al. 2018; Zhao et al. 2024).

Brain-derived proteins exhibited distinct temporal patterns, reflecting dynamic neuronal and glial responses. Astrocyte-specific markers GFAP and S100B peaked at PICU Day 1 and declined by PICU Day 3, consistent with 24- to 48-h biological half-lives (Huebschmann et al. 2020; Thelin et al. 2017). Tau pathology markers pTau-231 and pTau-181 followed a similar trajectory, peaking during the acute injury phase (Yadikar et al. 2025; Ashton et al. 2021; Munoz Pareja et al. 2024). In contrast, neurofilament proteins NEFH and NEFL demonstrated sustained elevation, potentially indicating progressive axonal structural damage (Gao et al. 2020; Theunissen et al. 2022; Coppens et al. 2023). Prior studies suggest neurofilament elevation can persist for months to years, enhancing their utility as chronic injury biomarkers (Tuure et al.

2024). Moreover, IL-6 in combination with NEFL/GFAP has previously demonstrated diagnostic utility for intracranial hemorrhage in the acute phase of TBI within 24 h of injury, further supporting their potential as early diagnostic biomarkers (Chiollaz et al. 2026). REST, a transcription factor that suppresses neuronal genes following injury (Kurschat et al. 2006), decreased from PICU Day 1 to PICU Day 3, potentially reflecting acute transcriptional remodeling. Conversely, NGF demonstrated sustained elevation, suggesting ongoing neuroprotective responses through attenuation of oxidative stress and inflammatory signaling, as well as enhancement of neuronal repair (Chiaretti et al. 2008, 2009; Zhou et al. 2003; Capossela et al. 2024). Decrease of CRH and TAFA5 at PICU Day 1 suggests hypothalamic dysfunction driven by inflammatory responses (Cammisa et al. 2025; Kang et al. 2020).

Network analysis revealed a prominent cluster centered on APP metabolism. Following axonal injury, APP colocalizes with processing enzymes BACE1 and PSEN1 (Uryu et al. 2007), which sequentially cleave APP to generate amyloid-β peptides (Cai et al. 2001; Bagaria et al. 2022). Although BACE1 was decreased, PSEN1 increase may drive altered enzymatic activity (Li et al. 2022). The observed decrease in plasma Aβ42 may reflect increased cerebral plaque deposition rather than reduced production (Franz et al. 2003), particularly given concurrent APOE increase, which promotes amyloid deposition via the E4 allele (Liu et al. 2017; Johnson et al. 2010). Increased abundance of MAPT alongside phosphorylated tau isoforms may indicate neurofibrillary pathology (Johnson et al. 2010; Edwards et al. 2020). Notably, TBI induces DNA methylation changes affecting genes encoding MAPT, APP, and neurofilaments (NEFL, NEFH) (Abu Hamdeh et al. 2021), suggesting epigenetic mechanisms may perpetuate protein accumulation and axonal damage beyond the acute phase.

A smaller peroxiredoxin/oxidative stress cluster comprised PRDX6, UCHL1, and PARK7, all increased in response to cellular damage. PRDX6, expressed primarily in astrocytes, hydrolyzes hydrogen peroxide (Buonora et al. 2015), though cerebrospinal fluid (CSF) PRDX6 oxidation in TBI patients raises questions about its functional capacity (Manevich et al. 2014). UCHL1 facilitates degradation of misfolded proteins (Diaz-Arrastia et al. 2014), while PARK7 repairs glycated proteins (Richarme et al. 2015), potentially enhancing antioxidant function through cysteine deglycation. Decrease of TEK, an endothelial receptor tyrosine kinase essential for vascular integrity (Khan et al. 2014), alongside decreased VEGF-D expression and increased VEGF-A, may reflect blood–brain barrier endothelial dysfunction (Stacker and Achen 2018). NPY, a neuroprotective factor promoting neurogenesis and attenuating inflammation (Zhang et al. 2021), was similarly decreased. CRH was also decreased, possibly reflecting glucocorticoid-mediated dysregulation following acute stress responses (Weil et al. 2022). Cellular component enrichment analysis demonstrated that DEPs were significantly annotated to neuronal, synaptic, cytoskeletal, and extracellular compartments, supporting the biological relevance of the identified proteomic signature to CNS injury. Importantly, these enrichments reflect annotation-based localization of proteins rather than direct evidence of compartment-specific injury, as plasma measurements cannot resolve cellular origin.

Exploratory correlation analyses between DEPs and clinical outcomes revealed detectable associations despite the modest sample size. On PICU Day 1, the inflammatory chemokines CCL2, CCL3, and CCL4 demonstrated coordinated positive correlations with mortality. These proteins share functional roles in monocyte and macrophage recruitment to sites of tissue damage, and their coordinated elevation is consistent with excessive early inflammation contributing to secondary injury cascades (Semple et al. 2010; Gyoneva and Ransohoff 2015; Ciechanowska et al. 2020).

MAPT demonstrated positive correlations with both mortality and brain herniation on PICU Day 1. By PICU Day 3, pTau-231 emerged as an integrative marker of secondary brain injury, correlating with herniation and bilaterally fixed pupils. Phosphorylated tau isoforms have garnered increasing interest as TBI biomarkers, with highly sensitive assays now enabling detection of pTau-181 and pTau-231 in plasma (Shahim et al. 2020; Shahim and Zetterberg 2022). Tau and phosphorylated tau levels have been shown to correlate with clinical and radiological variables of TBI severity and remain elevated for up to 90 days post-injury (Bogoslovsky et al. 2017). Our findings suggest that tau-based biomarkers may be particularly useful for identifying patients at risk of secondary injury progression in pediatric sTBI.

GFAP, which was mortality-associated on PICU Day 1, sustained positive correlation with death at PICU Day 3. This temporal pattern is consistent with GFAP kinetics, with concentrations increasing following injury and remaining elevated for up to 72 h (Abdelhak et al. 2022). In adult TBI, plasma GFAP measured on the day of injury has demonstrated good to excellent prognostic value for predicting death, with areas under the curve exceeding 0.76 (Lei et al. 2015; Korley et al. 2022).

TREM2 showed negative correlation with herniation at PICU Day 3 but not on PICU Day 1, suggesting delayed protective association. TREM2 is a microglial receptor that modulates neuroinflammation and promotes phagocytic clearance of cellular debris (Katsumoto et al. 2022). In experimental TBI models, TREM2 expression peaks at 3 days post-injury (Yan et al. 2022), and activation exerts

neuroprotective effects by inhibiting neutrophil infiltration and suppressing neuroinflammation (Yan et al. 2022; Li et al. 2024).

VEGF-D was the sole protein demonstrating negative correlation with mortality and positive correlation with rehabilitation discharge at PICU Day 1. While the VEGF family has complex and context-dependent roles in TBI pathophysiology (with VEGF-A contributing to both blood–brain barrier permeability and neuroprotective angiogenesis (Thau-Zuchman et al. 2010; Li et al. 2016)), VEGF-D specifically has been shown to be increased in pial vessels and inflammatory cells following brain injury (Nag et al. 2019). The protective association observed in our cohort may reflect preserved vascular repair capacity in patients with more favorable outcomes, though the precise mechanisms underlying VEGF-D's potential neuroprotective role in pediatric sTBI require further elucidation.

The detection of these protein-outcome associations in a limited exploratory cohort, particularly the emergence of functionally related protein clusters, suggests that some associations may be robust, though validation is required. The temporal evolution from broad inflammatory correlations on PICU Day 1 toward consolidated glial and tau signatures on PICU Day 3 carries implications for biomarker development, suggesting that optimal prognostic panels may be timepoint-dependent. Validation in larger, adequately powered cohorts is warranted to confirm reproducibility, establish whether these signals are specific to pediatric populations, and determine whether these molecular signatures can inform clinical prognostication or therapeutic stratification in pediatric sTBI.

Several limitations of our study warrant consideration. A primary limitation is the use of healthy controls, which limits the ability to distinguish TBI-specific changes from those due to systemic trauma, critical illness, or extracranial injuries. Many observed inflammatory signals likely reflect combined systemic and neurotrauma responses rather than exclusively brain-derived processes (Li et al. 2026). Several brain-associated proteins are also influenced by extracranial injury: S100B, though glial in origin, is expressed in adipocytes, melanocytes, and chondrocytes and can be elevated after fractures or soft tissue trauma (Anderson et al. 2001), while NSE is present in erythrocytes (Jungar et al. 2026). Future studies incorporating trauma-only (e.g., orthopedic) control groups and covariate adjustment for systemic insult markers will be important to disentangle CNS-specific from generalized trauma effects.

Another limitation of this study is incomplete paired sampling across the Day 3–5 window. Not all patients with Day 1 samples had a subsequent sample available, which may introduce attrition bias in longitudinal comparisons. Although PCA clustering supports proteomic consistency across this window, it cannot account for patients who were absent from later-timepoint sampling entirely. Furthermore, plasma collection beginning at PICU Day 1 limits characterization of the earliest acute-phase responses, particularly the oxidative stress- and DAMP-driven inflammatory surge occurring within the first 24 h of injury (Zhu et al. 2026). Observed proteomic trajectories are therefore biased toward structurally stable proteins with slower turnover kinetics—such as neurofilaments and GFAP—which accumulate gradually and persist in circulation over days. Earlier and more frequent sampling will be necessary to fully characterize the acute inflammatory proteomic landscape in pediatric sTBI.

The modest sample size and single-center design reflect the exploratory nature of this investigation and limit statistical power and generalizability, although cohort demographics align with larger pediatric sTBI populations. A limitation of this study is the biological heterogeneity introduced by the broad pediatric age range of the cohort. The plasma proteome changes substantially across childhood and adolescence owing to ongoing neurodevelopmental maturation and hormonal shifts; age may therefore act as a biological effect modifier of the post-injury proteomic response. Future studies with larger cohorts should include age as a covariate or incorporate age-stratified analyses. The CNS Disease Panel utilized primarily measures neuronal proteins, potentially missing unanticipated pathways and limiting the scope of pathway enrichment analyses. Plasma sampling, while minimally invasive and more feasible for downstream diagnostic/prognostic insight, may not fully reflect CNS parenchymal biology compared to CSF, particularly for brain-derived proteins subject to blood–brain barrier regulation. The absence of cell type-specific protein expression data limits characterization of cellular sources and pathophysiological mechanisms underlying observed changes. Finally, the lack of an independent validation cohort precludes confirmation of the reproducibility of these signatures. Future studies should incorporate larger multi-center cohorts with longitudinal sampling, assess for nutritional intake, comorbidity matching, extended outcome correlation (ex. GOS-E Peds scores), CSF analysis, and complementary omics platforms (transcriptomics, metabolomics) to validate these findings and advance toward clinically actionable biomarker panels for precision medicine in pediatric sTBI.

Conclusions

This exploratory study provides the first multi-domain proteomic characterization of severe pediatric traumatic brain injury using the NULISA platform. We identified 67 DEPs on PICU Day 1 spanning five neuropathologic

domains, with inflammation predominating. We demonstrated coherent temporal, network-level, and enrichment-based patterns that support biologically structured responses rather than isolated biomarker changes. STRING network analysis positioned IL-6 as a highly connected node, consistent with its known literature connectivity across inflammatory and neurodegeneration-related pathways, and suggesting coordinated activation of immune and neural injury programs in sTBI, while ten brain-associated proteins exhibited distinct temporal trajectories during the acute phase, underscoring the dynamic nature of early injury biology. Although the modest sample size and targeted panel limit definitive correlation analysis, these findings support the feasibility of plasma-based ultra-sensitive proteomics for capturing CNS-relevant molecular programs in pediatric sTBI and establish a systems-level framework for future validation studies.

Abbreviations

Aβ	Amyloid beta
ACHE	Acetylcholinesterase
AD	Alzheimer's disease
APOE	Apolipoprotein E
APP	Amyloid precursor protein
BACE1	Beta-site APP-cleaving enzyme 1
BBB	Blood–brain barrier
CCL	C–C motif chemokine ligand
CH-LHSC	Children's Hospital, London Health Sciences Centre
CNTN2	Contactin-2
CNS	Central nervous system
CRH	Corticotropin-releasing hormone
CRP	C-reactive protein
CSF	Cerebrospinal fluid
CST3	Cystatin C
CXCL	C–X–C motif chemokine ligand
DEPs	Differentially expressed proteins
DNA	Deoxyribonucleic acid
ENO2	Enolase 2
FC	Fold change
FDR	False discovery rate
GFAP	Glial fibrillary acidic protein
GCS	Glasgow Coma Scale
GO	Gene Ontology
ICU	Intensive care unit
IL	Interleukin
IQR	Interquartile range
ISS	Injury Severity Score
KLK6	Kallikrein related peptidase 6
MAIS	Maximum Abbreviated Injury Scale
MAPT	Microtubule-associated protein tau
MDH1	Malate dehydrogenase 1
MME	Membrane metalloendopeptidase
MSLN	Mesothelin
NEFH	Neurofilament heavy chain
NEFL	Neurofilament light chain
NGF	Nerve growth factor
NPTX1	Neuronal pentraxin-1
NPTXR	Neuronal pentraxin receptor
NPY	Neuropeptide Y
NULISA	Nucleic Acid-Linked Immuno-Sandwich Assay
PARK7	Parkinsonism associated deglycase
PCA	Principal component analysis
POSTN	Periostin
pTau	Phosphorylated tau
PICU	Pediatric intensive care unit
PPI	Protein–protein interaction
PRDX6	Peroxiredoxin-6
PSEN1	Presenilin-1
REST	RE1-silencing transcription factor
RNA	Ribonucleic acid
S100A12	S100 calcium binding protein A12
SAA1	Serum amyloid A1
SLIT2	Slit guidance ligand 2
SQSTM1	Sequestosome 1
sTBI	Severe traumatic brain injury
SMI	Sample-specific molecular identifier
SMOC1	SPARC related modular calcium binding 1
STRING	Search Tool for the Retrieval of Interacting Genes/Proteins
TAFA5	TAFA chemokine-like family member 5
TEK/TIE2	Endothelial tyrosine kinase receptor
TMI	Target-specific molecular identifier
TREM1	Triggering Receptor Expressed on Myeloid cells 1
TREM2	Triggering Receptor Expressed on Myeloid cells 2
UCHL1	Ubiquitin C-terminal hydrolase-L1
VEGF	Vascular endothelial growth factor

Supplementary Information

The online version contains supplementary material available at https://doi.org/10.1186/s10020-026-01501-9.

Supplementary Material 1.

Acknowledgements
Not applicable.

Authors' contributions
DDF conceived and designed the study. EC and DDF collected human samples and clinical data. EC, LRVN, DT, MD, MM, GC, and DDF analyzed all data and produced figures. DDF and LRVN provided content expertise and data review. EC, LRVN and DDF wrote the manuscript with input from all other authors.

Funding
DDF received study funding from the GSK Chair in Clinical Pharmacology (Western University, London, ON), a Legacy Gift via the Children's Health Foundation (https://childhealth.ca/) and the AMOSO Innovation Fund.

Data availability
The datasets generated and/or analyzed during the current study are available from the corresponding author upon reasonable request.

Declarations

Ethics approval and consent to participate
This study was approved by the Western University, Human Research Ethics Board (REB #s 6970; #100036; # 6963). Our experimental methods were performed in accordance with ethical standards of the responsible committee on human experimentation with the Helsinki Declaration of 1975. Informed written consent was obtained from either participants or their legal guardians.

Consent for publication
Not applicable.

Competing interests
The authors declare no competing interests.

Author details
[1]Physiology & Pharmacology, Western University, London, ON N6A 3K7, Canada
[2]Critical Care Medicine, Western University, London, ON, Canada
[3]Computer Science, Western University, London, ON N6A 3K7, Canada
[4]Epidemiology and Biostatistics, Western University, London, ON N6A 3K7, Canada

[5]Experimental Medicine, University of Rome Tor Vergata, Rome 00133, Italy
[6]Medical Biophysics, Western University, London, ON N6A 3K7, Canada
[7]Anatomy and Cell Biology, Western University, London, ON N6A 3K7, Canada
[8]London Health Sciences Centre Research Institute, London, ON N6C 2R5, Canada
[9]Pediatrics, Western University, London, ON N6A 3K7, Canada
[10]Clinical Neurological Sciences, Western University, London, ON N6A 3K7, Canada
[11]Children's Health Research Institute, London, ON N6C 4V3, Canada
[12]GSK Chair in Clinical Pharmacology, Western University, London, ON N6A 3K7, Canada

Received: 25 February 2026 / Accepted: 4 May 2026
Published online: 14 May 2026

References

Abdelhak A, Foschi M, Abu-Rumeileh S, Yue JK, D'Anna L, Huss A, et al. Blood GFAP as an emerging biomarker in brain and spinal cord disorders. Nat Rev Neurol. 2022;18(3):158–72.
Abeytunge K, Miller MR, Cameron S, Stewart TC, Alharfi I, Fraser DD, et al. Development of a mortality prediction tool in pediatric severe traumatic brain injury. Neurotrauma Rep. 2021;2(1):115–22.
Abu Hamdeh S, Ciuculete DM, Sarkisyan D, Bakalkin G, Ingelsson M, Schioth HB, et al. Differential DNA methylation of the genes for amyloid precursor protein, tau, and neurofilaments in human traumatic brain injury. J Neurotrauma. 2021;38(12):1679–88.
Åkerlund CA, Holst A, Bhattacharyay S, Stocchetti N, Steyerberg E, Smielewski P, et al. Clinical descriptors of disease trajectories in patients with traumatic brain injury in the intensive care unit (CENTER-TBI): a multicentre observational cohort study. Lancet Neurol. 2024;23(1):71–80.
Alharfi IM, Stewart TC, Kelly SH, Morrison GC, Fraser DD. Hypernatremia is associated with increased risk of mortality in pediatric severe traumatic brain injury. J Neurotrauma. 2013;30(5):361–6.
Alharfi IM, Charyk Stewart T, Al Helali I, Daoud H, Fraser DD. Infection rates, fevers, and associated factors in pediatric severe traumatic brain injury. J Neurotrauma. 2014;31(5):452–8.
Alofisan TO, Algarni YA, Alharfi IM, Miller MR, Charyk Stewart T, Fraser DD, et al. Paroxysmal sympathetic hyperactivity after severe traumatic brain injury in children: prevalence, risk factors, and outcome. Pediatr Crit Care Med. 2019;20(3):252–8.
Anderson RE, Hansson LO, Nilsson O, Dijlai-Merzoug R, Settergren G. High serum S100B levels for trauma patients without head injuries. Neurosurgery. 2001;48(6):1255–8 discussion 1258-1260.
Ashton NJ, Pascoal TA, Karikari TK, Benedet AL, Lantero-Rodriguez J, Brinkmalm G, et al. Plasma p-tau231: a new biomarker for incipient Alzheimer's disease pathology. Acta Neuropathol. 2021;141(5):709–24.
Bagaria J, Bagyinszky E, An SSA. Genetics, Functions, and Clinical Impact of Presenilin-1 (PSEN1) Gene. Int J Mol Sci. 2022;23(18):10970.
Bell MJ, Adelson PD, Hutchison JS, Kochanek PM, Tasker RC, Vavilala MS, et al. Differences in medical therapy goals for children with severe traumatic brain injury—an international study. Pediatr Crit Care Med. 2013;14(8):811–8.
Bogoslovsky T, Wilson D, Chen Y, Hanlon D, Gill J, Jeromin A, et al. Increases of plasma levels of glial fibrillary acidic protein, tau, and amyloid β up to 90 days after traumatic brain injury. J Neurotrauma. 2017;34(1):66–73.
Brisson AR, Matsui D, Rieder MJ, Fraser DD. Translational research in pediatrics: tissue sampling and biobanking. Pediatrics. 2012;129(1):153–62.
Buonora JE, Mousseau M, Jacobowitz DM, Lazarus RC, Yarnell AM, Olsen CH, et al. Autoimmune profiling reveals Peroxiredoxin 6 as a candidate traumatic brain injury biomarker. J Neurotrauma. 2015;32(22):1805–14.
Caceres E, Divani AA, Olivella-Gomez J, Di Napoli M, Reyes LF. Interleukin-6 and its association with outcome in traumatic brain injury: a prospective cohort. Scand J Trauma Resusc Emerg Med. 2025;33(1):131.
Cai H, Wang Y, McCarthy D, Wen H, Borchelt DR, Price DL, et al. BACE1 is the major beta-secretase for generation of Abeta peptides by neurons. Nat Neurosci. 2001;4(3):233–4.
Cammisa I, Malavolta E, Sodero G, Rigante D, Cipolla C. Endocrine Dysfunctions After Pediatric Traumatic Brain Injury: Present Insights and Future Directions. Children (Basel). 2025;12(11):1484.
Capossela L, Gatto A, Ferretti S, Di Sarno L, Graglia B, Massese M, Soligo M, Chiaretti A. Multifaceted Roles of Nerve Growth Factor: A Comprehensive Review with a Special Insight into Pediatric Perspectives. Biology (Basel). 2024;13(7):546.
Chen D, Tang TX, Deng H, Yang XP, Tang ZH. Interleukin-7 biology and its effects on immune cells: mediator of generation, differentiation, survival, and homeostasis. Front Immunol. 2021;12:747324.
Chen M, Ren AH, Prassas I, Soosaipillai A, Lim B, Fraser DD, et al. Plasma protein profiling by proximity extension assay technology reveals novel biomarkers of traumatic brain injury-a pilot study. J Appl Lab Med. 2021;6(5):1165–78.
Chen M, Soosaipillai A, Fraser DD, Diamandis EP. Discovery of novel plasma biomarker ratios to discriminate traumatic brain injury. F1000Res. 2019;8:1695.
Chiaretti A, Antonelli A, Riccardi R, Genovese O, Pezzotti P, Di Rocco C, et al. Nerve growth factor expression correlates with severity and outcome of traumatic brain injury in children. Eur J Paediatr Neurol. 2008;12(3):195–204.
Chiaretti A, Barone G, Riccardi R, Antonelli A, Pezzotti P, Genovese O, et al. NGF, DCX, and NSE upregulation correlates with severity and outcome of head trauma in children. Neurology. 2009;72(7):609–16.
Chiollaz AC, Pouillard V, Seiler M, Habre C, Romano F, Ritter Schenk C, et al. IL6 in combination with either NfL, NTproBNP, or GFAP to safely discharge children with mild traumatic brain injury. J Neurotrauma. 2026;43(3–4):248–58.
Ciechanowska A, Popiolek-Barczyk K, Pawlik K, Ciapala K, Oggioni M, Mercurio D, et al. Changes in macrophage inflammatory protein-1 (MIP-1) family members expression induced by traumatic brain injury in mice. Immunobiology. 2020;225(3):151911.
Coppens S, Lehmann S, Hopley C, Hirtz C. Neurofilament-light, a promising biomarker: analytical, metrological and clinical challenges. Int J Mol Sci. 2023;24(14):11624.
Cui M, Deng F, Disis ML, Cheng C, Zhang L. Advances in the clinical application of high-throughput proteomics. Explor Res Hypothesis Med. 2024;9(3):209–20.
Daley M, Cameron S, Ganesan SL, Patel MA, Stewart TC, Miller MR, et al. Pediatric severe traumatic brain injury mortality prediction determined with machine learning-based modeling. Injury. 2022;53(3):992–8.
Dewan MC, Mummareddy N, Wellons JC III, Bonfield CM. Epidemiology of global pediatric traumatic brain injury: qualitative review. World Neurosurg. 2016;91:497–509 e491.
Diaz-Arrastia R, Wang KK, Papa L, Sorani MD, Yue JK, Puccio AM, et al. Acute biomarkers of traumatic brain injury: relationship between plasma levels of ubiquitin C-terminal hydrolase-L1 and glial fibrillary acidic protein. J Neurotrauma. 2014;31(1):19–25.
Edwards G 3rd, Zhao J, Dash PK, Soto C, Moreno-Gonzalez I. Traumatic brain injury induces Tau aggregation and spreading. J Neurotrauma. 2020;37(1):80–92.
Erenler AK, Baydin A. Interleukin-33 (IL-33) as a diagnostic and prognostic factor in traumatic brain injury. Emerg Med Int. 2020;2020:1832345.
Farre-Alins V, Palomino-Antolin A, Narros-Fernandez P, Lopez-Rodriguez AB, Decouty-Perez C, Munoz-Montero A, Zamorano-Fernandez J, Mansilla-Fernandez B, Giner-Garcia J, Garcia-Feijoo P, et al. Serum Amyloid A1/Toll-Like Receptor-4 Axis, an Important Link between Inflammation and Outcome of TBI Patients. Biomedicines. 2021;9(6):599.
Feng MJ, Ning WB, Wang W, Lv ZH, Liu XB, Zhu Y, et al. Serum S100A12 as a prognostic biomarker of severe traumatic brain injury. Clin Chim Acta. 2018;480:84–91.
Feng W, Beer JC, Hao Q, Ariyapala IS, Sahajan A, Komarov A, et al. NULISA: a proteomic liquid biopsy platform with attomolar sensitivity and high multiplexing. Nat Commun. 2023;14(1):7238.
Figaji AA. Anatomical and physiological differences between children and adults relevant to traumatic brain injury and the implications for clinical assessment and care. Front Neurol. 2017;8:685.
Franz G, Beer R, Kampfl A, Engelhardt K, Schmutzhard E, Ulmer H, et al. Amyloid beta 1-42 and tau in cerebrospinal fluid after severe traumatic brain injury. Neurology. 2003;60(9):1457–61.
Fraser DD, Close TE, Rose KL, Ward R, Mehl M, Farrell C, et al. Severe traumatic brain injury in children elevates glial fibrillary acidic protein in cerebrospinal fluid and serum. Pediatr Crit Care Med. 2011;12(3):319–24.
Gao W, Zhang Z, Lv X, Wu Q, Yan J, Mao G, et al. Neurofilament light chain level in traumatic brain injury: a system review and meta-analysis. Medicine (Baltimore). 2020;99(38):e22363.
Garcia JM, Stillings SA, Leclerc JL, Phillips H, Edwards NJ, Robicsek SA, et al. Role of Interleukin-10 in acute brain injuries. Front Neurol. 2017;8:244.
Gillio-Meina C, Cepinskas G, Cecchini EL, Fraser DD. Translational research in pediatrics II: blood collection, processing, shipping, and storage. Pediatrics. 2013;131(4):754–66.

Gyoneva S, Ransohoff RM. Inflammatory reaction after traumatic brain injury: therapeutic potential of targeting cell-cell communication by chemokines. Trends Pharmacol Sci. 2015;36(7):471–80.
Hamza T, Barnett JB, Li B. Interleukin 12 a key immunoregulatory cytokine in infection applications. Int J Mol Sci. 2010;11(3):789–806.
Haqqani AS, Hutchison JS, Ward R, Stanimirovic DB. Protein biomarkers in serum of pediatric patients with severe traumatic brain injury identified by ICAT–LC-MS/MS. J Neurotrauma. 2007;24(1):54–74.
Haydel MJ, Weisbrod LJ, Saeed W. Pediatric Head Trauma. In: StatPearls. Treasure Island (FL): 2026. https://www.ncbi.nlm.nih.gov/books/NBK537029/
Hochstadter E, Stewart TC, Alharfi IM, Ranger A, Fraser DD. Subarachnoid hemorrhage prevalence and its association with short-term outcome in pediatric severe traumatic brain injury. Neurocrit Care. 2014;21(3):505–13.
Huang H, Fu G, Lu S, Chen S, Huo J, Ran Y, et al. Plasma profiles of inflammatory cytokines in children with moderate to severe traumatic brain injury: a prospective cohort study. Eur J Pediatr. 2024;183(8):3359–68.
Huebschmann NA, Luoto TM, Karr JE, Berghem K, Blennow K, Zetterberg H, et al. Comparing glial fibrillary acidic protein (GFAP) in serum and plasma following mild traumatic brain injury in older adults. Front Neurol. 2020;11:1054.
Hussain E, Prokop JW, Nonnemacher E, Ashrafi N, Yilmaz A, Mimi RA, Khalid A, Krinickis K, Lomeikaite V, Sanfilippo L. The molecular architecture of severe pediatric traumatic brain injury: integrated omics reveal therapeutic pathways. Critical Care. 2025;30(1):23.
Johnson VE, Stewart W, Smith DH. Traumatic brain injury and amyloid-beta pathology: a link to Alzheimer's disease? Nat Rev Neurosci. 2010;11(5):361–70.
Jullienne A, Obenaus A, Ichkova A, Savona-Baron C, Pearce WJ, Badaut J. Chronic cerebrovascular dysfunction after traumatic brain injury. J Neurosci Res. 2016;94(7):609–22.
Jungar C, Alinder E, Becker C, Moseby-Knappe M, Lybeck A. Hemolysis correction factor in the reporting of serum neuron-specific enolase - clinical utility in neuroprognostication after cardiac arrest. Resusc plus. 2026;28:101208.
Kang D, Kim HR, Kim KK, Kim DH, Jeong B, Jin S, et al. Brain-specific chemokine FAM19A5 induces hypothalamic inflammation. Biochem Biophys Res Commun. 2020;523(4):829–34.
Katsumoto A, Kokiko-Cochran ON, Bemiller SM, Xu G, Ransohoff RM, Lamb BT. Triggering receptor expressed on myeloid cells 2 deficiency exacerbates injury-induced inflammation in a mouse model of tauopathy. Front Immunol. 2022;13:978423.
Khan AA, Sandhya VK, Singh P, Parthasarathy D, Kumar A, Advani J, et al. Signaling network map of endothelial TEK tyrosine kinase. J Signal Transduct. 2014;2014:173026.
Kochanek PM, Tasker RC, Bell MJ, Adelson PD, Carney N, Vavilala MS, et al. Management of pediatric severe traumatic brain injury: 2019 consensus and guidelines-based algorithm for first and second tier therapies. Pediatr Crit Care Med. 2019;20(3):269–79.
Kolsto T, Werner D, Thorsen K, Weber C. Pediatric moderate and severe traumatic brain injury - a national, population-based cohort study. Eur J Trauma Emerg Surg. 2025;51(1):324.
Korley FK, Jain S, Sun X, Puccio AM, Yue JK, Gardner RC, et al. Prognostic value of day-of-injury plasma GFAP and UCH-L1 concentrations for predicting functional recovery after traumatic brain injury in patients from the US TRACK-TBI cohort: an observational cohort study. Lancet Neurol. 2022;21(9):803–13.
Kurschat P, Bielenberg D, Rossignol-Tallandier M, Stahl A, Klagsbrun M. Neuron restrictive silencer factor NRSF/REST is a transcriptional repressor of neuropilin-1 and diminishes the ability of semaphorin 3A to inhibit keratinocyte migration. J Biol Chem. 2006;281(5):2721–9.
Lassaren P, Lindblad C, Frostell A, Carpenter KLH, Guilfoyle MR, Hutchinson PJA, et al. Systemic inflammation alters the neuroinflammatory response: a prospective clinical trial in traumatic brain injury. J Neuroinflammation. 2021;18(1):221.
Lei J, Gao G, Feng J, Jin Y, Wang C, Mao Q, et al. Glial fibrillary acidic protein as a biomarker in severe traumatic brain injury patients: a prospective cohort study. Crit Care. 2015;19(1):362.
Li M, Jia Q, Chen T, Zhao Z, Chen J, Zhang J. The role of vascular endothelial growth factor and vascular endothelial growth inhibitor in clinical outcome of traumatic brain injury. Clin Neurol Neurosurg. 2016;144:7–13.
Li Z, Yu S, Li L, Zhou C, Wang L, Tang S, et al. TREM2 alleviates white matter injury after traumatic brain injury in mice might be mediated by regulation of DHCR24/LXR pathway in microglia. Clin Transl Med. 2024;14(4):e1665.
Li LM, Kodosaki E, Heslegrave A, Zetterberg H, Graham N, Zimmerman K, et al. High-dimensional proteomic analysis for pathophysiological classification of traumatic brain injury. Brain. 2025;148(3):1015–30.
Li LM, Kodosaki E, Xu CJY, Heslegrave A, Zetterberg H, Graham NSN, et al. Systemic inflammation and its associations in acute moderate-severe traumatic brain injury: a cross-sectional study. Brain Behav Immun Health. 2026;52:101179.
Li N, Qiu Y, Wang H, Zhao J, Qing H. PS1 Affects the Pathology of Alzheimer's Disease by Regulating BACE1 Distribution in the ER and BACE1 Maturation in the Golgi Apparatus. Int J Mol Sci. 2022;23(24):16151.
Lindblad C, Pin E, Just D, Al Nimer F, Nilsson P, Bellander BM, et al. Fluid proteomics of CSF and serum reveal important neuroinflammatory proteins in blood-brain barrier disruption and outcome prediction following severe traumatic brain injury: a prospective, observational study. Crit Care. 2021;25(1):103.
Liu CC, Zhao N, Fu Y, Wang N, Linares C, Tsai CW, et al. ApoE4 Accelerates Early Seeding of Amyloid Pathology. Neuron. 2017;96(5):1024–32 e1023.
Liu W, Taso O, Wang R, Bayram S, Graham AC, Garcia-Reitboeck P, et al. Trem2 promotes anti-inflammatory responses in microglia and is suppressed under pro-inflammatory conditions. Hum Mol Genet. 2020;29(19):3224–48.
Maas AIR, Menon DK, Manley GT, Abrams M, Akerlund C, Andelic N, et al. Traumatic brain injury: progress and challenges in prevention, clinical care, and research. Lancet Neurol. 2022;21(11):1004–60.
Manevich Y, Hutchens S, Halushka PV, Tew KD, Townsend DM, Jauch EC, et al. Peroxiredoxin VI oxidation in cerebrospinal fluid correlates with traumatic brain injury outcome. Free Radic Biol Med. 2014;72:210–21.
Marzano LAS, Batista JPT, de Abreu Arruda M, de Freitas Cardoso MG, de Barros JLVM, Moreira JM, et al. Traumatic brain injury biomarkers in pediatric patients: a systematic review. Neurosurg Rev. 2022;45(1):167–97.
McFadyen CA, Zeiler FA, Newcombe V, Synnot A, Steyerberg E, Gruen RL, et al. Apolipoprotein E4 polymorphism and outcomes from traumatic brain injury: a living systematic review and meta-analysis. J Neurotrauma. 2021;38(8):1124–36.
McKee CA, Lukens JR. Emerging roles for the immune system in traumatic brain injury. Front Immunol. 2016;7:556.
Miller AM. Role of IL-33 in inflammation and disease. J Inflamm (Lond). 2011;8(1):22.
Miller MR, Robinson M, Fischer L, DiBattista A, Patel MA, Daley M, et al. Putative concussion biomarkers identified in adolescent male athletes using targeted plasma proteomics. Front Neurol. 2021;12:787480.
Munoz Pareja JC, de Rivero Vaccari JP, Chavez MM, Kerrigan M, Pringle C, Guthrie K, et al. Prognostic and diagnostic utility of serum biomarkers in pediatric traumatic brain injury. J Neurotrauma. 2024;41(1–2):106–22.
Nag S, Manias J, Eubanks JH, Stewart DJ. Increased expression of vascular endothelial growth factor-D following brain injury. Int J Mol Sci. 2019;20(7):1594.
Niewold TB, Lehman JS, Gunnarsson I, Meves A, Oke V. Role of interleukin-16 in human diseases: a novel potential therapeutic target. Front Immunol. 2025;16:1524026.
Patel MA, Fraser DD, Daley M, Cepinskas G, Veraldi N, Grazioli S. The plasma proteome differentiates the multisystem inflammatory syndrome in children (MIS-C) from children with SARS-CoV-2 negative sepsis. Mol Med. 2024;30(1):51.
Richarme G, Mihoub M, Dairou J, Bui LC, Leger T, Lamouri A. Parkinsonism-associated protein DJ-1/Park7 is a major protein deglycase that repairs methylglyoxal- and glyoxal-glycated cysteine, arginine, and lysine residues. J Biol Chem. 2015;290(3):1885–97.
Riemann L, Zweckberger K, Unterberg A, El Damaty A, Younsi A, Collaborative European NeuroTrauma Effectiveness Research in Traumatic Brain Injury I, Participants. Injury causes and severity in pediatric traumatic brain injury patients admitted to the ward or intensive care unit: a collaborative European neurotrauma effectiveness research in traumatic brain injury (CENTER-TBI) study. Front Neurol. 2020;11:345.
Ryan E, Kelly L, Stacey C, Huggard D, Duff E, McCollum D, et al. Mild-to-severe traumatic brain injury in children: altered cytokines reflect severity. J Neuroinflammation. 2022;19(1):36.
Samanta RJ, Chiollaz AC, Needham E, Yue JK, Helmy A, Zanier ER, et al. Parsimonious immune-response endotypes and global outcome in patients with traumatic brain injury. EBioMedicine. 2024;108:105310.
Semple BD, Kossmann T, Morganti-Kossmann MC. Role of chemokines in CNS health and pathology: a focus on the CCL2/CCR2 and CXCL8/CXCR2 networks. J Cereb Blood Flow Metab. 2010;30(3):459–73.
Semple BD, Bye N, Rancan M, Ziebell JM, Morganti-Kossmann MC. Role of CCL2 (MCP-1) in traumatic brain injury (TBI): evidence from severe TBI patients and CCL2–/– mice. J Cereb Blood Flow Metab. 2010;30(4):769–82.
Serpa RO, Ferguson L, Larson C, Bailard J, Cooke S, Greco T, et al. Pathophysiology of pediatric traumatic brain injury. Front Neurol. 2021;12:696510.

Shahim P, Zetterberg H. Neurochemical markers of traumatic brain injury: relevance to acute diagnostics, disease monitoring, and neuropsychiatric outcome prediction. Biol Psychiatry. 2022;91(5):405–12.
Shahim P, Politis A, Van Der Merwe A, Moore B, Chou Y-Y, Pham DL, et al. Neurofilament light as a biomarker in traumatic brain injury. Neurology. 2020;95(6):e610–22.
Spagnolo P, Cela E, Patel MA, Tweddell D, Daley M, Clarson C, et al. Differential expression of plasma proteins and pathway enrichments in pediatric diabetic ketoacidosis. Mol Med. 2025;31(1):4.
Stacker SA, Achen MG. Emerging Roles for VEGF-D in Human Disease. Biomolecules. 2018;8(1):1.
Stewart TC, Alharfi IM, Fraser DD. The role of serious concomitant injuries in the treatment and outcome of pediatric severe traumatic brain injury. J Trauma Acute Care Surg. 2013;75(5):836–42.
Stocchetti N, Carbonara M, Citerio G, Ercole A, Skrifvars MB, Smielewski P, et al. Severe traumatic brain injury: targeted management in the intensive care unit. Lancet Neurol. 2017;16(6):452–64.
Stranges V, Tweddell D, Cela E, Morello M, Daley M, Cepinskas G, Fraser DD. Differential protein expression and enriched pathways in pediatric sepsis: identification of novel brain-associated biomarkers revealed through proteomic profiling. Mol Med. 2025;32(1):14.
Tenovuo O, Diaz-Arrastia R, Goldstein LE, Sharp DJ, van der Naalt J, Zasler ND. Assessing the Severity of Traumatic Brain Injury-Time for a Change? J Clin Med. 2021;10(1):148.
Thau-Zuchman O, Shohami E, Alexandrovich AG, Leker RR. Vascular endothelial growth factor increases neurogenesis after traumatic brain injury. J Cereb Blood Flow Metab. 2010;30(5):1008–16.
Thelin EP, Zeiler FA, Ercole A, Mondello S, Buki A, Bellander BM, et al. Serial sampling of serum protein biomarkers for monitoring human traumatic brain injury dynamics: a systematic review. Front Neurol. 2017;8:300.
Theunissen F, Anderton RS, Mastaglia FL, James I, Bedlack R, Akkari PA. Intronic NEFH variant is associated with reduced risk for sporadic ALS and later age of disease onset. Sci Rep. 2022;12(1):14739.
Tuure J, Mohammadian M, Tenovuo O, Blennow K, Hossain I, Hutchinson P, et al. Late blood levels of neurofilament light correlate with outcome in patients with traumatic brain injury. J Neurotrauma. 2024;41(3–4):359–68.
Uryu K, Chen XH, Martinez D, Browne KD, Johnson VE, Graham DI, et al. Multiple proteins implicated in neurodegenerative diseases accumulate in axons after brain trauma in humans. Exp Neurol. 2007;208(2):185–92.
Walker PA, Harting MT, Baumgartner JE, Fletcher S, Strobel N, Cox CS Jr. Modern approaches to pediatric brain injury therapy. J Trauma. 2009;67(2 Suppl):S120-127.
Wang ZY, Du W, Liu XZ, Li Y, Liu J. Elevation of C-reactive protein and homocysteine levels as reliable biomarkers for assessing injury severity and prognosis in traumatic brain injury. Sci Rep. 2025;15(1):18819.
Weil ZM, Karelina K. Lifelong consequences of brain injuries during development: from risk to resilience. Front Neuroendocrinol. 2019;55:100793.
Weil ZM, White B, Whitehead B, Karelina K. The role of the stress system in recovery after traumatic brain injury: a tribute to Bruce S. McEwen. Neurobiol Stress. 2022;19:100467.
Xanthos DN, Sandkühler J. Neurogenic neuroinflammation: inflammatory CNS reactions in response to neuronal activity. Nat Rev Neurosci. 2014;15(1):43–53.
Yadikar H, Kobeissy FH, Robertson C, Tsetsou S, Williamson JB, Lamb DG, et al. Early cerebrospinal fluid elevations of pTau-217 in severe traumatic brain injury subjects. Front Neurol. 2025;16:1632679.
Yan J, Zhang Y, Wang L, Li Z, Tang S, Wang Y, et al. TREM2 activation alleviates neural damage via Akt/CREB/BDNF signalling after traumatic brain injury in mice. J Neuroinflammation. 2022;19(1):289.
Zhang C, Chen S. Role of TREM2 in the development of neurodegenerative diseases after traumatic brain injury. Mol Neurobiol. 2023;60(1):342–54.
Zhang S, Xu Q. Proteomics reveals molecular subtypes in traumatic brain injury patients: new perspectives for precision treatment strategies. Front Immunol. 2025;16:1606268.
Zhang Y, Liu CY, Chen WC, Shi YC, Wang CM, Lin S, et al. Regulation of neuropeptide Y in body microenvironments and its potential application in therapies: a review. Cell Biosci. 2021;11(1):151.
Zhang Z, Yu J, Wang P, Lin L, Liu R, Zeng R, et al. iTRAQ-based proteomic profiling reveals protein alterations after traumatic brain injury and supports thyroxine as a potential treatment. Mol Brain. 2021;14(1):25.
Zhao T, Zhou Y, Zhang D, Han D, Ma J, Li S, et al. Inhibition of TREM-1 alleviates neuroinflammation by modulating microglial polarization via SYK/p38MAPK signaling pathway after traumatic brain injury. Brain Res. 2024;1834:148907.
Zhou Z, Chen H, Zhang K, Yang H, Liu J, Huang Q. Protective effect of nerve growth factor on neurons after traumatic brain injury. J Basic Clin Physiol Pharmacol. 2003;14(3):217–24.
Zhu L, Huang S, Chen W, Li K, Sheng J. Cytokines and related signaling pathways in traumatic brain injury. Front Immunol. 2026;17:1738589.
Žurek J, Fedora M. The usefulness of S100B, NSE, GFAP, NF-H, secretagogin and Hsp70 as a predictive biomarker of outcome in children with traumatic brain injury. Acta Neurochir. 2012;154(1):93–103.

Publisher's Note

Springer Nature remains neutral with regard to jurisdictional claims in published maps and institutional affiliations.